

NASA TECHNICAL NOTE



NASA TN D-3230

NASA TN D-3230



RECEIVED  
KOTLAND AFB

AN EXPERIMENTAL INVESTIGATION OF  
HEAT TRANSFER TO TURBULENT FLOW  
IN SMOOTH TUBES FOR  
THE REACTING  $N_2O_4$ - $NO_2$  SYSTEM

*by Alden F. Presler*  
*Lewis Research Center*  
*Cleveland, Ohio*





AN EXPERIMENTAL INVESTIGATION OF HEAT TRANSFER TO  
TURBULENT FLOW IN SMOOTH TUBES FOR THE  
REACTING  $N_2O_4$ - $NO_2$  SYSTEM

By Alden F. Presler

Lewis Research Center  
Cleveland, Ohio

NATIONAL AERONAUTICS AND SPACE ADMINISTRATION

---

For sale by the Clearinghouse for Federal Scientific and Technical Information  
Springfield, Virginia 22151 - Price \$2.00

AN EXPERIMENTAL INVESTIGATION OF HEAT TRANSFER TO TURBULENT FLOW IN  
SMOOTH TUBES FOR THE REACTING  $N_2O_4$ - $NO_2$  SYSTEM

by Alden F. Presler

Lewis Research Center

SUMMARY

Local turbulent heat-transfer coefficients were obtained experimentally for the dissociating system  $N_2O_4$ - $NO_2$  flowing through an electrically heated tube. For these experiments the tube length to diameter ratio was 40. Experimental conditions covered a seven-fold increase in the uniform heat flux up to 44 000 Btu per hour per square foot and an eight-fold increase in mass average velocity up to 130 000 pounds per hour per square foot. The maximum tube wall temperatures ranged from 359° to 572° K.

Modified local heat-transfer coefficients, based on wall- to bulk-enthalpy differences, were correlated very well as a simple power of the mass average velocity.

The local modified heat-transfer coefficients were correlated with a Dittus-Boelter-Colburn-type relation with all equilibrium transport and thermal properties evaluated on a mean temperature integral basis. The best curve through the data was about ten percent below the curve from constant property analyses.

INTRODUCTION

The absorption of the heat of chemical reaction by a dissociating gas is somewhat analogous to the absorption of the heat of vaporization of a boiling liquid in that both fluids act as effective heat sinks. For this reason a number of gases have recently been examined as potential heat-transfer fluids, particularly for special applications in cooling of nuclear reactors (ref. 1).

In a heat-transfer process the effect of a chemical reaction is most apparent in the unusual sensitivity of the fluid thermal conductivity and specific heat to changes in temperature and pressure. Calculation of these properties is very difficult except when the products and reactants are in chemical equilibrium. For this special condition the expressions for the thermal conductivity and specific heat are relatively simple and tractable (ref. 2).

Of the possible equilibrium chemical reactions, the gaseous system  $\text{N}_2\text{O}_4 \rightleftharpoons 2\text{NO}_2$  has been most attractive for heat-transfer studies because its interesting thermophysical properties can be exploited in experiments within the temperature range  $300^\circ$  to  $500^\circ$  K and at pressures of 1 to 2 atmospheres. The gas can also be obtained and stored in suitably pure form. The  $\text{N}_2\text{O}_4$  system was used in the present experiment because of both the previous reasons and the recent reported study of its transport properties (ref. 3), which gave necessary data for the correlations.

The large variations of thermal properties in a reacting system provide a severe test for the standard turbulent flow heat-transfer correlations, which have usually been derived for constant property fluids. The purpose of the present experiment was to provide extensive heat-transfer data for the turbulent flow in a tube of a gas in chemical equilibrium and with these data check some of the correlations that have been devised to account for deviations from the constant property assumptions in the analyses.

In the present experiments the heat exchange was from an electrically heated tube to turbulent flows of  $\text{N}_2\text{O}_4$ - $\text{NO}_2$  gas. The experimental conditions covered a seven-fold increase in the uniform heat flux up to 44 000 Btu per hour per square foot and an eight-fold increase in the mass average velocity up to 130 000 pounds per hour per square foot. The tube wall temperatures were adjusted to provide wall properties with maximum chemical reaction effects for the low wall temperature runs and wall properties due to the completely dissociated gas for the highest wall temperature runs. The experiments were designed to give the largest variations in the important heat-transfer variables and parameters as was possible with the equipment.

Sources of data from previous investigations of the  $\text{N}_2\text{O}_4$  turbulent heat-transfer system are listed in table I. References 4 to 7 reported experimental results with uniform wall temperature conditions. These experiments are characterized by relatively modest values of wall heat flux.

The other references in table I are concerned with heat transfer under uniform heat flux conditions. The data of reference 8 were taken at the very short length to diameter ratio of 2 and were only later correlated (ref. 9) using a Colburn-type equation and more complete thermophysical property data.

Two companion papers (refs. 10 and 11) considered radial variations in properties in correlating the data with both Deissler's analogy (ref. 12) and with Colburn's analogy (ref. 13, p. 424). There was fair agreement between theory and experiment.

More general discussions of reacting systems with heat transfer, and with emphasis on boundary layer flows, have been presented by Spalding (ref. 14) and Knuth (ref. 15).

## SYMBOLS

$A_{f1}$	cross-sectional flow area, sq ft
$A_w$	inside heated wall area, sq ft
$\hat{C}_p$	mass basis specific heat, Btu/(lb)(°F)
$\hat{C}_{p,e}$	mass basis equilibrium specific heat, Btu/(lb)(°F)
$\overline{\hat{C}}_{p,e}$	mean temperature integral specific heat, Btu/(lb)(°F)
$\hat{C}_{p,f}$	mass basis frozen specific heat, Btu/(lb)(°F)
$\hat{C}_{p,r}$	mass basis reactive specific heat defined by eq. (A27)
$D$	inside tube diameter, ft
$\mathcal{D}$	binary diffusion coefficient, sq ft/hr
$E$	electrical potential, V
$\Delta F^\circ$	standard state Gibbs' free energy, cal/g mole
$f$	friction factor
$G$	mass velocity, $W/A_{f1}$ , lb/(sq ft)(hr)
$H^\circ$	standard state molar enthalpy, cal/g mole
$\Delta H^\circ$	standard state heat of reaction, cal/g mole
$\Delta H_F^\circ$	standard state heat of formation, cal/g mole
$h$	heat-transfer coefficient based on wall to bulk temperature difference, Btu/(hr)(sq ft)(°F)
$h'$	modified heat-transfer coefficient based on wall to bulk enthalpy difference, lb/(hr)(sq ft)
$I$	electrical current, A
$i$	mass basis enthalpy, Btu/lb
$j_H$	Colburn factor, $St'(Pr_e)^{2/3}$
$K_p$	equilibrium constant for $N_2O_4$ system, atm

$k_e$	equilibrium thermal conductivity, Btu/(hr)(sq ft)(°F/ft)
$\bar{k}_e$	mean temperature integral thermal conductivity, Btu/(hr)(sq ft)(°F/ft)
$k_f$	frozen property thermal conductivity, Btu/(hr)(sq ft)(°F/ft)
$k_r$	reactive contribution to thermal conductivity, eq. (A30)
$L$	heated tube length, ft
$M$	molecular weight of equilibrium gas mixture, lb/lb mole
$M_{\text{NO}_2}$	molecular weight of $\text{NO}_2$ molecule, 46.008 lb/lb mole
$M_{\text{N}_2\text{O}_4}$	molecular weight of $\text{N}_2\text{O}_4$ molecule, 92.016 lb/lb mole
$\mathcal{M}$	mass fraction of species
$m$	coefficient in eq. (7)
$\text{Nu}$	standard Nusselt number, $hD/k_f$ or $hD/k_e$
$\text{Nu}'$	modified Nusselt number, $h'D/\Gamma_e$
$\overline{\text{Nu}}'$	modified Nusselt number based on mean temperature integral equilibrium properties, $h'D/\overline{\Gamma}_e$
$n$	number of fillings of test loop in eq. (1)
$P$	absolute total pressure, atm
$\text{Pr}$	Prandtl number, $\mu/\Gamma$
$\text{Pr}_e$	Prandtl number based on equilibrium properties, $\mu/\Gamma_e = \hat{\mu}_{p,e}/k_e$
$\overline{\text{Pr}}_e$	Prandtl number based on mean temperature integral equilibrium properties, $\overline{\mu}/\overline{\Gamma}_e$
$\text{Pr}_f$	Prandtl number based on frozen properties, $\mu/\Gamma_f$
$p$	absolute partial pressure, atm
$Q$	rate of electrical heat input, Btu/hr
$q$	heat flux to gas, Btu/(hr)(sq ft)

R universal gas constant

Re Reynolds number,  $GD/\mu$

$\overline{Re}$  Reynolds number based on mean temperature integral viscosity,  $GD/\overline{\mu}$

St' modified Stanton number,  $Nu'/Re Pr_e$  or  $h'/G$

T temperature,  $^{\circ}K$

U bulk velocity,  $G/\rho_b$ , ft/hr

W mass flow rate, lb/hr

x distance from entrance of heated test section, ft

y mol fraction, mole/mole mixture

$\alpha$  degree of dissociation of initial 1 mol  $N_2O_4$ , mole/mole

$\Gamma$  thermal exchange coefficient,  $k/\hat{C}_p$

$\Gamma_e$  equilibrium thermal exchange coefficient,  $k_e/\hat{C}_{p,e}$ , lb/(ft)(hr)

$\overline{\Gamma}_e$  mean temperature integral equilibrium thermal exchange coefficient,  $\overline{k_f}/\hat{C}_{p,e}$ , lb/(ft)(hr)

$\Gamma_f$  frozen thermal exchange coefficient,  $k_f/\hat{C}_{p,f}$ , lb/(ft)(hr)

$\mu$  dynamic viscosity, lb/(ft)(hr)

$\overline{\mu}$  mean temperature integral dynamic viscosity, lb/(ft)(hr)

$\rho$  mixture density, lb/cu ft

$\phi$  general transport property in eq. (17)

$\chi$  Boltzmann factor,  $1.4384 \omega/T$

$\omega$  wave number,  $cm^{-1}$

Subscripts:

b bulk

e equilibrium

f frozen, or constant composition

mix mixture

P refers to properties at constant pressure

ref reference (indicates evaluation of properties at reference temperature  $T_{ref}$  or at temperature corresponding to reference enthalpy  $i_{ref}$ )

w wall

0 refers to property at absolute zero temperature

Superscript:

— mean temperature integral property

## APPARATUS AND PROCEDURE

### Flow System

The apparatus formed a closed flow loop containing a compressor, two rotameters, an electrically heated test section, and water-cooled heat exchangers as basic elements. The system is shown schematically in figure 1. The entire rig, exclusive of the control panels, was enclosed within a fume hood fitted with Lucite panels.

The compressor had a rated capacity of 17.0 standard cubic feet per minute at a maximum pressure rise of 15 pounds per square inch gage.

Two rotameters connected in parallel provided the gas flow rate indication. With both rotameters fully open the maximum indicated flow rate was 279 pounds per hour of  $N_2O_4$  gas at a standard density of 0.385 pound per cubic foot.

Two sets of jacketed heat exchangers, one upstream and the other downstream of the compressor, were fitted with both cold and hot water inputs so that the cooling water temperature could always be kept above the dew point of the test gas in the loop to avoid condensation.

### Power Supply

Electrical power to the test section was supplied by a regulated saturable core reactor with a rated capacity of 25 kilovolt amperes and a maximum output of 10 volts at 60 cycles on the transformer secondary.

### Test Section

Details of the test section and mixing boxes are given in figure 2. The test section was a tube of 347 stainless steel, with a 0.500-inch outside diameter, 0.404-inch inside diameter, and an overall length of 20 inches between mixing box flanges. The first 4 inches of the test section were unheated. Two pressure taps were provided on the test section, one on the upstream electrical

connection, and the other on the exit flange. The mixing boxes were constructed basically as three concentric cylindrical cans, which provided four abrupt turns with the mixing of the fluid stream. The mixing tanks were fabricated from 347 stainless-steel sheet.

Although not shown in figures 1 and 2, a 20-inch-long transite tube,  $3\frac{3}{4}$ -inch inside diameter, was fitted around the test section between the entrance and exit flanges. The annular space between the test section and the transite tube was filled with loose insulation. The transite tube was cut in half longitudinally so that it could be fit around the test section. Test section thermocouple leads were also brought out through the longitudinal joint.

### Instrumentation

Temperatures were sensed with 24-gage iron-constantan thermocouples and were recorded on a flight recorder. Thermocouples were swaged in sealed stainless-steel sheaths where direct contact with the gas was necessary (e.g., at the two rotameters), in the inlet and outlet of the compressor, and in the mixing tank gas streams at the inlet and outlet to the test section.

Bare thermocouples were spot welded to the outside of the test section, as is indicated in figure 2. These were usually put on in pairs, on the top and bottom, at any one longitudinal position. Each individual wire was looped once around the test section, and was held off the tube surface with insulating beads, before being brought out to a junction box. Five thermocouples in the middle 6 inches of the heated test section were alternated top and bottom. In total there were 30 thermocouples on the test section, and 22 on the transite insulating shell. The thermocouples on the transite shells were evenly distributed along its length, alternating top and bottom.

In addition to the flight recorder, thermocouple temperatures were indicated on a precision potentiometer in conjunction with an electronic null point indicator. The potentiometer temperatures were taken relative to the ice point. However, it was also possible to take temperature differences directly with the potentiometer. These more precise readings were used only for the crucial mixing tank and rotameter temperatures.

It is indicated in figure 1 that static pressures at the rotameter inlets and at the test section were obtained on manometers. Pressures at the inlet and outlet of the compressor were not needed with much precision and thus were monitored by stainless steel Bourdon gages.

All static pressure tubing was of 1/8-inch thinwall 347 stainless steel and was always attached to the top of the stainless drip pots. These pots were necessary to trap any gas from the system that may have condensed at the ambient temperatures. This ensured that the manometer lines were always free of liquid.

The gravity pots separating the manometers from the drip pots, which are shown in the lower right-hand corner of figure 1, were a later addition to the equipment to deal with the problem of  $\text{NO}_2$  gas entering and reacting with the

manometer fluids. These gravity pots, two in number in each manometer line, were welded stainless-steel cans about  $6\frac{1}{2}$  inches high and  $2\frac{1}{2}$  inches in diameter. Each set of pots in series functioned as a trap for the  $\text{NO}_2$  gas because the gas had a density of about three times that of air at the ambient conditions of the experimental runs.

Pressure drops across the test section were obtained with a differential manometer.

The voltage drops across the test section were measured directly on laboratory precision voltmeters. Current was measured by a conventional technique: an ammeter in conjunction with a current transformer having a ratio of 160. A wattmeter was also used with the voltmeter and ammeter as a check on their accuracy.

### Corrosion Problems

Special precautions were necessary to counter corrosion by gaseous  $\text{NO}_2$ . The flow loop was constructed as far as it was possible of glass or stainless steel. Gaskets were constructed from sheet Teflon, and all screwed fittings were doped with a Teflon-water paste; rotameter tube washers were machined from Teflon rod; compressor shaft seals and bearings were lubricated with Kel-F oil.

The cast iron body of the compressor and the plastic vanes of the rotor were not attacked by the gas. However, the compressor had to be operated dry (i.e., without any vane lubricant) after a number of oils apparently were polymerized and degraded by the gas.

All bare iron-constantan thermocouple junctions corroded on first contact with the gas. Thereafter, it was necessary that all thermocouple probes in direct contact with the gas be constructed with the thermocouple wires swaged in sealed stainless-steel sheaths.

### Filling and Operation

Filling the test loop with the  $\text{NO}_2$  gas was accompanied by the purging of the air in the system. This was accomplished by the pulling of a modest vacuum on the system followed by filling of the loop to some specified pressure from a small pressurized supply bottle of  $\text{NO}_2$  exterior to the system. The supply bottle was not stored in the vicinity of the rig, and is not shown in figure 1. Running the compressor for 10 minutes after a system filling with  $\text{NO}_2$  was considered sufficient to thoroughly mix the  $\text{NO}_2$  gas with residual air in the loop. Each cycle of evacuation, filling, and mixing reduced the mole fraction of residual air in the system.

Since the equipment was always filled to the same pressure and evacuated

to the same pressure, then the mole fraction of residual air after  $n$  cycles was

$$y_n = \left(\frac{p}{P}\right)^n \quad (1)$$

That the air was rapidly exhausted from the system can be seen from a numerical example. The loop was typically exhausted to 25 inches of vacuum (i.e.,  $p \approx 5/30 = 1/6$  atm abs) and filled to 2 atmospheres absolute. Then after 3 cycles

$$y_3 = \left(\frac{1}{2} \frac{1}{6}\right)^3 = 0.00058$$

This number represents a nominal impurity of 0.058 mole percent after 3 cycles, which is well within the 99.5 weight percent minimum assay claimed for the cylinder gas (ref. 16).

After the filling operation, power was applied to the test section for a given gas flow rate and the test section with its blanket of insulation was allowed to come to thermal equilibrium, which usually required 4 to 5 hours. The compressor shaft seals never worked perfectly and allowed a small but steady leak of  $\text{NO}_2$  gas into the fume hood. This meant that an equivalent amount of  $\text{N}_2\text{O}_4$  was constantly fed to the system in order to maintain constant pressure.

The water temperature in the cooling jackets of the heat exchangers was adjusted according to the vapor pressure curve given in figure 3. For a given system pressure, the temperatures at all points in the loop had to be at values above the vapor pressure curve. This put a lower limit on the amount of cooling of gas from the hot test section, and a limit on the amount of recooling of the gas heated in the compressor. The penalty for having liquid  $\text{N}_2\text{O}_4$  in the loop was flow and temperature surges.

A chemical analysis or assay of the oxides of nitrogen in the system was made during the time that the rig was coming to thermal equilibrium prior to a run. The complete procedure for the assay is given in reference 16. Only a resume will be sketched here.

Three clean, dry glass balloons (e.g., Guillard bulbs) of about 500-milliliter capacity were evacuated and weighed on an analytical balance. The bulbs were filled with gas from the test loop to about 1-atmosphere pressure and then weighed again. A measured amount of a dilute  $\text{H}_2\text{O}_2$  solution was forced into the bulbs. This oxidized any lower nitrogen oxides to  $\text{NO}_2$ , and this gas dissolved in the solution to give  $\text{HNO}_3$ . The bulbs were opened, and the acid was decanted and washed into Erlenmeyer flasks where it was titrated to a methyl red endpoint with standard 0.2N NaOH reagent. The amount of  $\text{HNO}_3$  determined in each Guillard bulb, expressed on a weight basis as  $\text{NO}_2$ , was related on a percent basis to the total weight of original gas sample. The accuracy of the analysis was not exceptional, about 0.2 percent. However, the assay indicated that air was essentially exhausted from the system, for the weight percent of  $\text{NO}_2$  was never lower than 99.5, which was the minimum manufacturer's specification.

## DATA REDUCTION AND CORRELATION

The raw data from the experiments consisted of the voltage and current readings; the indicated temperatures at the rotameters, mixing boxes, test section walls, and transite insulation walls; the barometric pressure; the manometer pressures for the rotameters and the ends of the test section; and the indicated rotameter readings. The total power dissipated in the test section was

$$Q = (3.143)(160)EI \quad (2)$$

where the voltage  $E$  and current  $I$  were values corrected with meter calibration curves.

Overall heat loss was obtained by comparing the integral mean wall temperature with the corresponding mean temperature from the static heat loss tests. This provided a corrected heat input,

$$Q_{\text{corr}} = Q - Q_{\text{loss}}$$

This value was compared with the total enthalpy rise of the test gas between the mixing boxes to obtain a check on the heat balance,

$$\text{Heat balance error (percent)} = \frac{Q_{\text{corr}} - W(i_{b,\text{exit}} - i_{b,\text{inlet}})}{Q_{\text{corr}}} \times 100 \quad (3)$$

Temperatures on the inside of the wall were calculated from the external thermocouple readings using equation (1) of reference 17. The maximum temperature drop through the wall was  $3^{\circ}$  K, which occurred at the maximum heat input of 6240 Btu per hour. A summary of the important experimental test data is given in table II.

From equation (2) of reference 17, the heat input to the test gas was computed from

$$Q = W(i_{b,\text{exit}} - i_{b,\text{inlet}}) \quad (4)$$

and these are the values which have been given in table II. The bulk enthalpy-rise values of heat input were used in subsequent calculations. The measured electrical heat inputs were subjected to nonsinusoidal variations in waveform of the power supply. These waveform variations did not affect the bulk temperature rise, but they did give trouble in the recording of the electrical meter readings. The erratic waveform was the principal reason for the variations in the heat balance error recorded in table II.

The double thermocouple probes in each mixing box agreed to within  $0.1^{\circ}$  R for all tests, which was also the estimated accuracy of measurement of these temperatures.

The test rig was given a preliminary checkout of procedure and accuracy

with air as the test gas. The excellent results obtained, which proved the equipment, have been briefly reported elsewhere (ref. 18).

### PROPERTIES

The methods used to compute the thermodynamic and transport properties of the gaseous  $N_2O_4$  system are discussed in the appendix.

The magnitude of the effect of the chemical reaction on the thermal conductivity and specific heat of the gas mixture can be seen from the analytical values in figures 4 and 5. The difference between the "frozen" (i.e., constant composition) and equilibrium curves is the measure of the effect of reaction. The effect diminishes rapidly at higher temperatures where the system is essentially dissociated to  $NO_2$ .

The absolute enthalpy of the system, shown in figure 6, exhibits an inflection point at about  $340^\circ K$  for the case of  $P = 2$  atmospheres. As can be deduced from the material in the appendix, this represents the neighborhood of the maxima for the equilibrium  $k_e$  and  $\hat{C}_{p,e}$ .

Dynamic viscosity of the system, shown in figure 7, is much less affected by the presence of chemical reaction. It is, however, composition dependent as can be seen by the two analytical curves for one and two atmospheres. In this regard viscosity behavior is very similar to that of frozen thermal conductivity. In fact, the methods of computation of  $k_F$  and  $\mu$  are similar.

The thermal exchange coefficient  $\Gamma$  and Prandtl number  $Pr$  shown in figures 8 and 9, respectively, are properties derived after their respective components have been computed.

### DATA CORRELATION

The conventional correlation of fully developed turbulent flow heat transfer in a tube is the Dittus-Boelter equation (ref. 19).

$$\frac{hD}{k} = a \left( \frac{\rho U D}{\mu} \right)^b \left( \frac{C_p \mu}{k} \right)^c \quad (5)$$

For a uniform heat flux to a nonreactive fluid, the fully developed heat-transfer condition has a constant heat-transfer coefficient

$$h = \frac{q_w}{T_w - T_b} \quad (6)$$

which demands the  $T_w - T_b$  term be constant.

Humble (ref. 17) and Weiland (ref. 20) have discussed the important problem of choosing the temperature at which the transport properties are calcula-

ted for use in equation (5). Wall and bulk temperatures are the most convenient to obtain, while the best results seem to come from the use of a reference temperature defined by

$$T_{\text{ref}} = T_b + m(T_w - T_b) \quad (7)$$

with the value of  $m$  usually around 0.5 for nonreactive gases (ref. 13, p. 393).

The uniform heat flux of equation (6) can be related to the mixing box temperatures by

$$Q = qA_w = W \overline{\hat{C}_{p,b}} (T_{b,\text{exit}} - T_{b,\text{inlet}}) \quad (8)$$

where

$$\overline{\hat{C}_{p,b}} = \frac{1}{L} \int_0^L \hat{C}_{p,b} dx \quad (9)$$

Equation (8) is equivalent to the enthalpy expression

$$Q = W(i_{b,\text{exit}} - i_{b,\text{inlet}}) \quad (10)$$

provided that the correct specific heats are used in equation (9). For a chemical equilibrium situation like the present  $N_2O_4$  system, the use of frozen  $\hat{C}_{p,f}$  in equation (9) can give values of predicted  $Q$  from equation (8) that are almost an order of magnitude lower than the actual measured heat input.

Since equilibrium enthalpies must be used in equation (10) to reconstruct the measured heat inputs, it is consistent also to make use of the wall- to bulk-enthalpy difference,  $i_w - i_b$ , instead of the usual temperature difference,  $T_w - T_b$ , in the definition of the heat-transfer coefficient (eq. (6)). This will define a modified heat-transfer coefficient.

By analogy to equation (6), a modified heat-transfer coefficient can be defined by

$$h' = \frac{q_w}{i_w - i_b} \quad (11)$$

The relation between  $h'$  and  $h$  is from the ratio

$$\frac{h'}{h} = \frac{T_w - T_b}{i_w - i_b} \quad (12)$$

Equation (12) has the units of reciprocal specific heat.

The Nusselt number with the modified heat-transfer coefficient is now defined as

$$\text{Nu}' = h'D / \frac{k}{\bar{C}_p} \quad (13)$$

or

$$\text{Nu}' = \frac{h'D}{\Gamma} \quad (14)$$

where the thermal exchange coefficient

$$\Gamma = \frac{k}{\bar{C}_p}$$

The modified  $\text{Nu}'$  can be used in the Dittus-Boelter equation

$$\text{Nu}' = a \text{Re}^b \text{Pr}_e^c \quad (15)$$

where all transport properties must be calculated on the equilibrium basis. This correlation still retains the problem of determining the best reference temperature for calculating the properties. Besides the reference temperature defined by equation (7), reference enthalpies as

$$i_{\text{ref}} = i_b + m(i_w - i_b) \quad (16)$$

can be used to estimate a mean reference or film temperature. An analytical study on variable property turbulent heat transfer to nonreactive gases showed that equation (16) can be used very effectively with the usual  $\text{Nu-Re}$  correlation (ref. 12).

Brokaw (ref. 9) suggested the use of mean integral properties, which were calculated from the expression

$$\bar{\phi} = \frac{1}{T_w - T_b} \int_{T_b}^{T_w} \phi(T) dT \quad (17)$$

where  $\phi(T)$  represents any thermal or transport property. It was found that integral mean properties provided the best correlation for the data of Beal and Lyerly (ref. 8).

The data of this report was correlated by the Dittus-Boelter relation with

both standard and modified Nusselt numbers. The rearranged equation

$$\left(\frac{\text{Nu}'}{\text{Pr}_e}\right)^{1/3} = a \text{Re}^b \quad (18)$$

was the form used to test the data. The value of the Prandtl exponent in equation (15) has been taken to be  $1/3$  in equation (18).

For correlations with the modified Nusselt number the Reynolds number was taken as

$$\text{Re} = \frac{\text{GD}}{\mu} \quad (19)$$

where the viscosity was calculated at a specified reference temperature. For a Reynolds number defined by equation (19), the modified Stanton number has the particularly simple form

$$\text{St}' = \frac{\text{Nu}'}{\text{Re Pr}}$$

or

$$\text{St}' = \frac{h'}{G} \quad (20)$$

The  $\text{St}'$  of equation (20) has a definite advantage as a heat-transfer parameter since it contains no terms whose values depend on the choice of the film temperature.

From equation (15),

$$\text{St}' = a \text{Re}^{b-1} \text{Pr}_e^{-2/3} \quad (21)$$

Colburns' analogy (ref. 13, p. 424) follows directly from this

$$j'_H = \text{St}' \text{Pr}_e^{2/3} = a \text{Re}^{b-1} \quad (22)$$

$$j'_H = \frac{f}{2} \quad (23)$$

where the Blasius friction factor expression

$$f = 0.079 \text{Re}^{-1/4} \quad (24)$$

was used in the present work (ref. 13, p. 171).

## RESULTS AND DISCUSSION

The correlated test results of the air data are shown in figure 10. The purpose of these runs was to check out the instrumentation and the methods of data reduction.

Plots of wall temperatures for one air run and one run of the  $N_2O_4$  system are shown in figure 11. This pair of results was chosen because of similar mass rates of flow. It illustrates the profound effect of chemical reaction on heat transfer to a gas, for the frozen specific heat of the gaseous  $N_2O_4$  system is essentially that for air at moderate temperatures, and the system would have similar temperature curves to the air run were it not for the presence of the reaction  $N_2O_4 \rightleftharpoons 2NO_2$ . In this case, the  $N_2O_4$  system absorbed about twice the heat flux as the air system, and with a significantly lower wall temperature distribution and bulk temperature rise.

A criterion for fully developed heat transfer is a constant wall- to bulk-enthalpy difference. This is demonstrated in figure 12 for the same  $N_2O_4$  run that was used in figure 11. It was obviously impossible to choose, from the  $(T_w - T_b)$  curve, a point on the tube where fully developed heat transfer was established. The enthalpy difference curve indicated that fully developed heat transfer was established at the thermocouple position at 6.75 inches on the test section. This point corresponded to an  $x/D = 7.69$ . The constant property analysis of reference 21, for a Reynolds number of 50 000, found that a heated length of about 12 tube diameters was required to bring the local Nusselt number to within 5 percent of the fully developed value, and about 25 diameters to approach within 1 percent of fully established heat transfer. It should also be noted that the longitudinal temperature gradients at the entrance to the heated tube (fig. 11) were not as severe for the reacting system and affected a shorter length of tube than did the air runs.

A conventional heat-transfer correlation of the experimental data is given in figure 13. These are the runs of table II. The abnormally large Nu arises from the use of the low values of  $k_f$  and the anomalies of the conventional heat-transfer coefficient defined by equation (6). Since figure 12 demonstrated that a conventional heat-transfer coefficient would not be constant in the reacting system, it was necessary to arbitrarily choose a thermocouple position within the fully developed region from which the necessary temperature data could be obtained; in figure 13 all data were computed from temperatures at the tube position of 17.63 inches ( $x/D = 34.6$ ).

Figure 13 also indicates that the conventional correlation deviates more from the analytical result of reference 21 as the experimental wall temperatures diminished. This is in part due to the approach of the proper equilibrium thermal conductivity  $k_e$  to the limiting value of  $k_f$  at higher temperature (fig. 6) and in part due to the mean specific heat

$$\overline{\hat{C}}_{p,e} = \frac{1}{T_w - T_b} \int_{T_b}^{T_w} \hat{C}_{p,e} dT \quad (25)$$

approaching the frozen  $\hat{C}_{p,f}$  for large  $T_w$  as in figure 5.

Figures 14 to 16 illustrate the variation of equilibrium specific heat that occurred in the data for the three levels of wall temperatures. This spread of property variables over the three groups of experiments was deliberately planned, as mentioned in the INTRODUCTION, to give the widest possible variation in chemical effects at the wall.

The conventional correlation of the data with the equilibrium thermal conductivity  $k_e$  used in the Nusselt number has been given in figure 17. There the results for each run have been given at tube positions of 13.75 and 17.63 inches ( $x/D = 25.0$  and  $34.6$ , respectively). The contrast between these results and those in figure 13 is quite clear: the Nusselt numbers with  $k_e$  calculated at the wall temperature and those with  $k_e$  calculated at the bulk temperature, are essentially mirror images with respect to the region of the two analytical curves for constant properties. The choice of wall or bulk temperature made little difference in the Nusselt numbers of figure 13, but in figure 17 it had a most profound effect.

The other contrast observed between the two figures was the reversal of the positions of the low and high wall temperature Nusselt numbers relative to the analytical curve for constant properties.

The Nu, Re, and Pr functions were also calculated at temperatures corresponding to reference enthalpy positions of  $m = 0.3, 0.4, 0.5,$  and  $0.6$  in equation (16). The values for  $m = 0.6$  were much closer to the known analytical results for constant properties, and they have been plotted in figure 17 between the analytical curve for  $Pr = 1.0$  (ref. 22), and the curve for  $Pr = 0.7$  (ref. 23). The comparison of these data with the analytical curves is quite good.

The basic results from the experimental runs are summarized in table III. The heat flux  $q$ , the enthalpy difference  $i_w - i_b$ , and the modified heat-transfer coefficient  $h'$ , were invariant in the fully developed heat-transfer region of the tube, and subsequent correlations have made use of these data for this reason.

The comparison of the modified heat-transfer coefficient  $h'$  with the mass average velocity for the data of table III, and for the data of references 8 and 9 is shown in figure 18. Of the data reported in table III, fourteen runs were plotted within  $\pm 6$  percent of the correlation

$$h' = 0.00596 G^{0.884} \quad (26)$$

and of the four remaining runs, the high wall temperature series had deviations of 10 and 20 percent, the moderate wall temperature series had one of -22 percent, and the low wall temperature series had one of 8 percent deviation.

The data of Beal and Lysterly (ref. 8) and Callaghan and Mason (ref. 5) for uniform wall temperature systems have been used for figure 18. Local heat-transfer coefficients and data were recalculated to furnish the modified coefficients used in the figure. The data of Beal and Lysterly show the most deviation from the correlating curve, and this is probably because their measurements were taken at the extremely short heating length  $L/D = 2$ .

The success of equation (26) in correlating the  $N_2O_4$  data is rather surprising because it does not depend at all on any transport properties such as those used in the conventional Dittus-Boelter formulation (eq. (5)). It must again be emphasized here that the dissociation data plotted in figure 18 exhibited the widest possible variation of chemical effects on the properties of the system.

A correlation somewhat similar to equation (26) was independently investigated by Simoneau and Hendricks (ref. 24) for data on air, helium, hydrogen, and carbon dioxide, with rather large wall- to bulk-temperature differences. Their formulation can be written as

$$h \propto G^{0.8} \sqrt{\frac{T_b}{T_w}} \quad (27)$$

that is, in terms of the standard heat-transfer coefficient (eq. (6)).

Simoneau and Hendricks found that a different proportionality constant for equation (27) was needed with each of the four nonreactive gases. This behavior is analogous to the situation between the air and  $N_2O_4$  data in figure 18, where the form of equation (26) holds also for the air data, but a change in the value of the coefficient is necessary to shift the correlating line upward to enclose the air data points.

Correlation of the experimental data by equation (18) has been shown in figures 19 to 21 for  $Pr_e$ ,  $\Gamma_e$ , and  $\mu$  evaluated at local bulk and wall temperatures, and as integral mean values between the local wall and bulk temperatures.

Of the three correlating curves plotted in the figures, the ones due to Deissler (ref. 22) and Sparrow, et al. (ref. 21) are for constant property analyses.

Callaghan and Mason (ref. 5) found that equation (18) with  $a = 0.018$  and  $b = 0.8$  gave a good fit to their data over their limited range of Reynolds numbers. It is seen that their equation gave the best correlation for the present data over the extended Reynolds number range for any of the three bases of property calculations.

The considerable scatter in the wall-based data of figure 20 is due to the extreme differences in the wall temperatures between the three sets of data of the present experiment. The properties at the wall for the highest  $T_w$  runs were essentially those of frozen composition, and this was especially true for the sections of the tubes where fully developed heat transfer was established. Figures 14 to 16 demonstrate that there was far less variation in the bulk properties among the three data sets than in the wall properties. This was reflected in the better correlation on a bulk basis as is shown in figure 19.

The data correlation with the equilibrium properties calculated with equation (17) are shown in figure 21. This correlation is demonstrably superior to the previous ones of figures 19 and 20.

For Reynolds numbers in the range  $Re = 10^4$  to  $10^5$  the equation

$$\frac{Nu'}{Pr_e^{1/3}} = 0.018 Re^{0.8} \quad (27)$$

predicts values for the  $Nu'/Pr_e^{1/3}$  term that are about 25 percent lower than those using the equation of Sparrow, Hallman, and Siegel (ref. 21). This latter equation was shown in figure 10 to correlate the air data tests very nicely. Thus the air and  $N_2O_4$  data discrepancy of figure 18 has been carried over into the Nusselt number correlation. A probable explanation of this is that these correlations are somewhat inadequate approximations to the basic heat-transfer processes that occurred within the reacting system.

Results of correlating the data by the Colburn analogy of equations (22) and (23) are shown in figures 22 to 24. Comparison has been made with the analytical data of Deissler, and with the two empirical curves of figures 19 to 21, all having been transformed to the Colburn factor  $j_H$ . With  $Pr_e$  and  $Re$  based on bulk or wall temperatures, figures 22 and 23 show considerable data scatter in Colburn factors with these bases. Figure 24 shows the correlation derived with integral mean properties. The agreement with the bottom correlating curve is fairly good, especially if the four divergent data points discussed with figure 18 are discarded.

The exact Colburn analogy (eq. (23)), is plotted on figures 22 to 24 as one-half of the Blasius friction factor (eq. (24)). Deissler's analysis for  $Pr = 1.0$  is most closely approximated by the exact analogy.

The previous figures show that the experimental  $N_2O_4$ - $NO_2$  heat-transfer data can be correlated with a Dittus-Boelter-Colburn-type relationship and with regard to the use of the correct heat-transfer coefficient and thermal properties. That the correlation does not conform to the results of constant property analyses is at least in part due to the assumption of the Prandtl number entering the relation as a simple power. Sparrow, Hallman, and Siegel (ref. 21) had earlier concluded on the basis of analytical studies that the Prandtl number does not have such a simple power form. Petukhov and Popov (ref. 25) came to a similar conclusion after studying a large number of experi-

mental data from unreactive gases with property variations.

### CONCLUDING REMARKS

The following results were obtained in the investigation of local heat-transfer coefficients in the turbulent flow of gaseous  $N_2O_4$ - $NO_2$  through an electrically heated tube:

1. No consistent data correlation was obtained using the conventional Dittus-Boelter heat-transfer equation with frozen properties and with the standard heat-transfer coefficient based on the wall- to bulk-temperature difference.
2. Good agreement with constant property analyses was obtained when experimental Nusselt numbers were computed from reference equilibrium thermal conductivities and the standard heat-transfer coefficient and when reference equilibrium Prandtl numbers were used for the system. This correlation was very sensitive to the correct reference point, which was found to be at the temperature corresponding to the reference enthalpy  $i_{ref} = 0.6(i_w - i_b) + i_b$ .
3. A simple logarithmic correlation of the experimental modified heat-transfer coefficient  $h'$ , which was independent of transport properties, with the mass average velocity  $G$  was surprisingly good. A similar correlation was possible with local air data, but values of  $h'$  were about 18 percent higher than the dissociation result.
4. For each experimental run, the local modified heat-transfer coefficient  $h'$  based on local wall- to bulk-enthalpy differences was constant over the fully developed region of the test section. The local standard heat-transfer coefficient  $h$  based on local wall- to bulk-temperature differences, continuously decreased along the tube in the flow direction. Conversely, by using the constant value  $h'$  as the definition of fully developed heat transfer, the thermal entrance length for the dissociating system was found to be about half that predicted from analysis for constant property fluids.
5. Local Colburn factors  $Nu'/Pr_e^{1/3}$  were computed from the experimental modified heat-transfer coefficients  $h'$  and properties evaluated at three reference points: wall temperature, bulk temperature, and the mean temperature integral of the properties. Of these, the integral mean properties provided the most consistent data correlation, which agreed well with the expression  $\overline{Nu'}/\overline{Pr_e}^{1/3} = 0.018 \overline{Re}^{0.8}$ .
6. The Colburn analogy was shown to hold quite well for Deissler's constant property analysis with Prandtl number of unity, but the correlation of the experimental  $N_2O_4$ - $NO_2$  data, with integral mean properties, was quite good with the expression  $St' \overline{Pr_e}^{2/3} = 0.018/\overline{Re}^{0.2}$  which predicts values of the Colburn  $j_H$  factor about 20 percent less than those of Deissler's constant property analysis.

7. The Dittus-Boelter-Colburn heat-transfer correlation of the present experimental data, as well as of those of other investigations using  $N_2O_4$ - $NO_2$  gas, was consistently lower in magnitude than the same correlation for constant property analytical data.

Lewis Research Center,  
National Aeronautics and Space Administration,  
Cleveland, Ohio, November 2, 1965.

## APPENDIX - PROPERTY CALCULATIONS

### Degree of Dissociation

Determination of the degree of dissociation in the gas at any point in the test section was necessary for all further calculations of densities, and thermodynamic and transport properties. The basis of the calculation is the equilibrium constant expressed in terms of the partial pressures of the reactants and products

$$K_p = \frac{P_{\text{NO}_2}^2}{P_{\text{N}_2\text{O}_4}} \quad (\text{A1})$$

For a Dalton's Law system the partial pressures are products of the total system pressure  $P$  and the molar fractions of the constituents

$$\left. \begin{aligned} P_{\text{NO}_2} &= y_{\text{NO}_2} P \\ P_{\text{N}_2\text{O}_4} &= y_{\text{N}_2\text{O}_4} P \end{aligned} \right\} \quad (\text{A2})$$

and

where  $y_{\text{NO}_2} + y_{\text{N}_2\text{O}_4} = 1$  by definition. For an initial 1 mole of  $\text{N}_2\text{O}_4$ , the equilibrium composition has, for  $\alpha$  mole fraction of  $\text{N}_2\text{O}_4$  decomposed,  $(1 - \alpha)$  moles of  $\text{N}_2\text{O}_4$  remaining and  $2\alpha$  moles of  $\text{NO}_2$  formed from the  $\text{N}_2\text{O}_4$ . There are then  $(1 - \alpha) + 2\alpha = (1 + \alpha)$  moles in the equilibrium mixture; hence,

$$\left. \begin{aligned} y_{\text{NO}_2} &= \frac{2\alpha}{1 + \alpha} \\ y_{\text{N}_2\text{O}_4} &= \frac{1 - \alpha}{1 + \alpha} \end{aligned} \right\} \quad (\text{A3})$$

and

From the aforementioned expressions the equilibrium constant in terms of the degree of dissociation is

$$K_p = \frac{4\alpha^2 P}{1 - \alpha} \quad (\text{A4})$$

In terms of the equilibrium constant and the system pressure, the degree of dissociation is

$$\alpha = \sqrt{\frac{K_p}{4P + K_p}} \quad (A5)$$

Equation (A5) was the basis for all calculations of the degree of dissociation.

At the standard temperature 298.16° K (25° C) the equilibrium constant can be calculated from the standard state Gibbs' free energy, since (ref. 26, pp. 334, 349)

$$-\frac{\Delta F^\circ}{T} = R \ln K_p \quad (A6)$$

The necessary thermodynamic data is given in reference 31.

Extension of the equilibrium constant calculation to temperatures above 298.16° K was accomplished by integration of the van't Hoff isobar (ref. 26, p. 338).

$$\left(\frac{\partial \ln K_p}{\partial T}\right)_P = \frac{\Delta H^\circ}{RT^2} \quad (A7)$$

The standard enthalpy of reaction  $\Delta H^\circ$  at 298.16° K was obtained from reference 27. Variation in the  $\Delta H^\circ$  at higher temperatures, due to molar specific heat changes, was calculated by the method outlined in the section Enthalpies of this appendix.

The empirical equation

$$\log_{10} K_p = 9.218 - \frac{3006}{T} \quad (A8)$$

was found to give an excellent fit to the equilibrium constant data up to 490° K. At higher temperatures the agreement was somewhat less successful, but the gas was also almost completely dissociated at these temperatures and for the pressures encountered in the experiments.

The equilibrium constant increased rapidly with increasing temperature from a value of 0.157 at 300° K to 1180 at 490° K. Equation (A5) shows that large values of  $K_p$  result in values of  $\alpha$  approaching unity.

#### Mixture Densities

An ideal mixture of perfect gases obeys the perfect gas law

$$\rho = \frac{PM}{RT} \quad (A9)$$

where  $M$  is the average molecular weight of the mixture, that is,

$$M = y_{\text{NO}_2} M_{\text{NO}_2} + y_{\text{N}_2\text{O}_4} M_{\text{N}_2\text{O}_4} \quad (\text{A10})$$

for the  $\text{N}_2\text{O}_4$  gas system. Since  $M_{\text{N}_2\text{O}_4} = 2M_{\text{NO}_2}$ , equations (A3) and (A10) give for the mixture

$$M = \frac{M_{\text{N}_2\text{O}_4}}{1 + \alpha} \quad (\text{A11})$$

From equations (A9) and (A11), the mixture density is

$$\rho = \frac{PM_{\text{N}_2\text{O}_4}}{RT(1 + \alpha)} \quad (\text{A12})$$

### Enthalpies

The ideal gas enthalpies of a nonlinear polyatomic molecule are calculated from

$$\frac{H^\circ - H_0^\circ}{T} = 4R + R \sum_j \frac{\chi_j}{e^{\chi_j} - 1} \quad (\text{A13})$$

where the  $\chi_j = 1.4384 \omega_j/T$  and the summation is over all observed wave numbers (ref. 28). This reference gives the numbers for the  $\text{NO}_2$  and  $\text{N}_2\text{O}_4$  molecules as listed in table IV.

The molar enthalpies of the two molecules are

$$\left( \frac{H^\circ - H_0^\circ}{T} \right)_{\text{NO}_2} = 4R + R \sum_{j=1,2,3} \frac{\chi_j}{e^{\chi_j} - 1} \quad (\text{A14})$$

and

$$\left( \frac{H^\circ - H_0^\circ}{T} \right)_{\text{N}_2\text{O}_4} = 5R + R \sum_{j=1,\dots,6,8,\dots,12} \frac{\chi_j}{e^{\chi_j} - 1} \quad (\text{A15})$$

The additional  $R$  in the  $\text{N}_2\text{O}_4$  expression arises from the equipartition of

energy for the  $j = 7$  line, since that wave number is essentially zero in value. From this, for  $x_7 \cong 0$ ,

$$\lim_{x_j \rightarrow 0} \frac{x_j}{e^{x_j} - 1} = 1$$

The enthalpy of reaction at a temperature  $T$  is the difference between the summation over the product enthalpies and the summation over the reactant enthalpies (ref. 29). For the system  $N_2O_4 \rightleftharpoons 2NO_2$  the molar reaction enthalpy is

$$\Delta H^\circ = 2H_{NO_2}^\circ - H_{N_2O_4}^\circ \quad (A16)$$

Expressing the right-hand side of equation (A16) in terms of the respective relative enthalpies (ref. 29) gives the molar enthalpy of reaction as

$$\begin{aligned} \Delta H^\circ &= 2 \left[ (H^\circ - H_O^\circ) + \Delta H_{f,0}^\circ \right]_{NO_2} - \left[ (H^\circ - H_O^\circ) + \Delta H_{f,0}^\circ \right]_{N_2O_4} \\ &= 2(H^\circ - H_O^\circ)_{NO_2} - (H^\circ - H_O^\circ)_{N_2O_4} + 2(\Delta H_{f,0}^\circ)_{NO_2} - (\Delta H_{f,0}^\circ)_{N_2O_4} \end{aligned} \quad (A17)$$

The molar heats of formation at  $0^\circ$  K are given in reference 27 as the following for  $NO_2$ :

$$\Delta H_{f,0}^\circ = 8.682 \text{ kcal/mole}$$

and for  $N_2O_4$ :

$$\Delta H_{f,0}^\circ = 4.489 \text{ kcal/mole}$$

The  $(H^\circ - H_O^\circ)$  terms in equation (A17) are calculated with equations (A14) and (A15). Enthalpies of the gas mixture on a unit mass basis were calculated from

$$i_{\text{mix}} = \mathcal{M}_{NO_2} i_{NO_2} + \mathcal{M}_{N_2O_4} i_{N_2O_4} \quad (A18)$$

where in terms of the degree of dissociation of  $N_2O_4$  the mass fractions of the species are

$$\mathcal{M}_{NO_2} = \alpha, \quad \mathcal{M}_{N_2O_4} = 1 - \alpha \quad (A19)$$

The specific enthalpies of the individual species (i.e., enthalpies on a unit mass basis) are readily obtained from equations (A14), (A15), and (A17) as

$$\begin{aligned}
i_{\text{NO}_2} &= \frac{H_{\text{NO}_2}^{\circ}}{M_{\text{NO}_2}} \\
&= \frac{1}{M_{\text{NO}_2}} \left[ (H^{\circ} - H_0^{\circ}) + \Delta H_{f,0}^{\circ} \right]_{\text{NO}_2}
\end{aligned} \tag{A20}$$

and

$$\begin{aligned}
i_{\text{N}_2\text{O}_4} &= \frac{H_{\text{N}_2\text{O}_4}^{\circ}}{M_{\text{N}_2\text{O}_4}} \\
&= \frac{1}{M_{\text{N}_2\text{O}_4}} \left[ (H^{\circ} - H_0^{\circ}) + \Delta H_{f,0}^{\circ} \right]_{\text{N}_2\text{O}_4}
\end{aligned} \tag{A21}$$

Equation (A18) was the basis for enthalpy calculations with the experiment together with equations (A19) to (A21).

#### Specific Heats

The specific heat on a mass basis of the reacting gas mixture is derived from the specific enthalpy (eq. (A18)) in the usual manner

$$\hat{C}_{p,e} = \left( \frac{\partial i_{\text{mix}}}{\partial T} \right)_P \tag{A22}$$

$$\hat{C}_{p,e} = \alpha \left( \frac{\partial i_{\text{NO}_2}}{\partial T} \right)_P + (1 - \alpha) \left( \frac{\partial i_{\text{N}_2\text{O}_4}}{\partial T} \right)_P + i_{\text{NO}_2} \left( \frac{\partial \alpha}{\partial T} \right)_P - i_{\text{N}_2\text{O}_4} \left( \frac{\partial \alpha}{\partial T} \right)_P \tag{A23}$$

The terms on the right-hand side of equation (A23) are evaluated from equations (A19) to (A21). This results in

$$\hat{C}_{p,e} = \alpha \hat{C}_{p,\text{NO}_2} + (1 - \alpha) \hat{C}_{p,\text{N}_2\text{O}_4} + \frac{\Delta H_R^{\circ}}{M_{\text{N}_2\text{O}_4}} \left( \frac{\partial \alpha}{\partial T} \right)_P \tag{A24}$$

$$\hat{C}_{p,e} = \hat{C}_{p,f} + \hat{C}_{p,r} \tag{A25}$$

where the "frozen" (i.e., constant composition) specific heat is

$$\hat{C}_{p,f} = \alpha \hat{C}_{p,NO_2} + (1 - \alpha) \hat{C}_{p,N_2O_4} \quad (A26)$$

and the reactive specific heat is

$$\hat{C}_{p,r} = \frac{\Delta H^\circ}{M_{N_2O_4}} \left( \frac{\partial \alpha}{\partial T} \right)_P \quad (A27)$$

The gradient of the degree of dissociation with temperature at constant pressure uses equations (A5) and (A7) for the derivation. It can be shown from equations (A4) and (A7) that

$$\left( \frac{\partial \alpha}{\partial T} \right)_P = \frac{\alpha}{2} (1 - \alpha^2) \frac{\Delta H^\circ}{RT^2} \quad (A28)$$

so that the reactive component of specific heat becomes

$$\hat{C}_{p,r} = \frac{1}{2M_{N_2O_4}} \alpha (1 - \alpha^2) \quad (A29)$$

Equations (A24) and (A28) were those used to compute the experimental specific heats.

#### Thermal Conductivity

Experimental thermal conductivities of gaseous  $N_2O_4$  have been measured by Coffin and O'Neal (ref. 3). These values were shown to agree with analytical data calculated with the method of Butler and Brokaw (ref. 2). These authors showed that the thermal conductivity of a gaseous system in chemical equilibrium could be expressed as the sum of a frozen conductivity and a reactive conductivity, the latter representing the diffusional transport of the enthalpy of reaction

$$k_e = k_f + k_r \quad (A30)$$

Reference 2 showed that the reaction term

$$k_r = \left[ \frac{\partial P}{\partial T} \frac{\Delta H^\circ}{RT^2} \right] \frac{\alpha}{2} (1 - \alpha) \quad (A31)$$

The term in brackets is independent of pressure and its values between 290° K and 490° K have been tabulated by Coffin and O'Neal (ref. 3).

The frozen (i.e., constant composition) contribution to thermal conduc-

tivity is expressed as a sum of two terms

$$k_f = k' + k'' \quad (\text{A32})$$

where  $k'$  accounts for the collisional transport of translational kinetic energy of the species in the mixture and  $k''$  accounts for the diffusional transport of internal energy. The forms of these two terms are somewhat involved, and references 30 and 31 should be consulted for details. Reference 30 is especially recommended, although it is based on the treatise of Hirschfelder, et al. (ref. 31). The frozen contribution to thermal conductivities needed for this experiment were calculated from the equations of reference 8, and the force constant data for the  $\text{NO}_2$  and  $\text{N}_2\text{O}_4$  molecules were taken from table I of that reference.

The reactive contribution was calculated with equation (A31). Values of the term  $(\mathcal{O}P/RT)(\Delta H^{O2}/RT^2)$  in equation (A31) were interpolated from the data of Coffin and O'Neal (ref. 3). In order to extrapolate their data beyond  $490^\circ\text{K}$  the following empirical expression was used:

$$\frac{\mathcal{O}P}{RT} \frac{\Delta H^{O2}}{2} = \frac{2.756}{T} \frac{1.201}{T} \quad (\text{A33})$$

#### Viscosities

The viscosity of the gaseous  $\text{N}_2\text{O}_4$  system was calculated with equation (13) of reference 30. The form of this equation is similar to that for computing the  $k''$  term in the frozen thermal conductivity. As with the thermal conductivity calculations, the force constants of the  $\text{NO}_2$  and  $\text{N}_2\text{O}_4$  molecules were obtained from table I of reference 30.

Three sets of data are recorded on the viscosity plot of figure 7. The data of reference 7 is most certainly in error. The more recent data of Beer (ref. 32) shows the most discrepancy at the lower temperatures; the data of Petker and Mason (ref. 33) collected with a rolling-ball viscometer, parallels the curve of Brokaw (ref. 18), but with a discrepancy of 15 percent at  $450^\circ\text{K}$ .

## REFERENCES

1. McKisson, R. L.: Dissociation-Cooling: A Discussion. Rept. No. LRL-86, Calif. Res. and Dev. Co., Mar. 1954.
2. Butler, James N.; and Brokaw, Richard S.: Thermal Conductivity of Gas Mixtures in Chemical Equilibrium. J. Chem. Phys., vol. 26, no. 6, June 1957, pp. 1636-1643.
3. Coffin, Kenneth P.; and O'Neal, Cleveland, Jr.: Experimental Thermal Conductivities of the  $N_2O_4 \rightleftharpoons 2NO_2$  System. NACA TN 4209, 1958.
4. Schotte, William: Heat Transfer to a Gas-Phase Chemical Reaction. Ind. Eng. Chem., vol. 50, no. 4, Apr. 1958, pp. 683-690.
5. Callaghan, Michael J.; and Mason, David M.: Momentum and Heat Transfer Correlations for a Reacting Gas in Turbulent Pipe Flow. A.I.Ch.E. J., vol. 10, no. 1, Jan. 1964, pp. 52-55.
6. Krieve, Walter F.; and Mason, David M.: Heat Transfer in Reacting Systems: Heat Transfer to Nitrogen Dioxide Gas Under Turbulent Pipe Flow Conditions. A.I.Ch.E. J., vol. 7, no. 2, June 1961, pp. 277-281.
7. Thievon, William J.; Sterbutzel, Gerald A.; and Beal, John L.: The Influence of Gas Dissociation on Heat Transfer. Rept. No. TR-59-450, WADC, June 1959.
8. Beal, John L.; and Lyerly, Ray L.: The Influence of Gas Dissociation on Heat Transfer. Rept. No. Tr 56-494, WADC, Sept. 1956.
9. Brokaw, Richard S.: Correlation of Turbulent Heat Transfer in a Tube for the Dissociating System  $N_2O_4 \rightleftharpoons 2NO_2$ . NACA RM E57K19a, 1958.
10. Irving, J. P.; and Smith, J. M.: Heat Transfer in a Chemically Reacting System (Nitrogen Tetroxide-Dioxide). A.I.Ch.E. J., vol. 7, no. 1, Mar. 1961, pp. 91-96.
11. Furgason, R. R.; and Smith, J. M.: Heat Transfer in the Nitrogen Dioxide-Nitrogen Tetroxide System. A.I.Ch.E. J., vol. 8, no. 5, Nov. 1962, pp. 654-658.
12. Deissler, Robert G.; and Presler, Alden F.: Computed Reference Temperatures for Turbulent Variable Property Heat Transfer in a Tube for Several Common Gases. Int. Dev. in Heat Transfer, Pt. III, ASME, 1961, pp. 579-584.
13. Knudsen, James G.; and Katz, Donald L.: Fluid Dynamics and Heat Transfer. McGraw-Hill Book Co., Inc., 1958.
14. Spalding, D. B.: Heat Transfer from Reacting Systems. Modern Developments in Heat Transfer, W. E. Ibele, ed., Academic Press, 1963, pp. 19-64.

15. Knuth, Eldon: Recent Studies on the Use of Reference States in Predicting Transport Rates for High-Speed Flows with Mass Transfers. Proc. 1963 Heat Transfer and Fluid Mech. Inst., Stanford Univ. Press, 1963, pp. 27-43.
16. Anon.: Nitrogen Tetroxide. Nitrogen Div. Product Bull., Allied Chem. Co., 1960.
17. Humble, Leroy V.; Lowdermilk, Warren H.; and Desmon, Leland G.: Measurements of Average Heat-Transfer and Friction Coefficients for Subsonic Flow of Air in Smooth Tubes at High Surface and Fluid Temperatures. NACA Rept. 1020, 1951.
18. Siegel, R.; and Sparrow, E. M.: Turbulent Flow in a Circular Tube with Arbitrary Internal Heat Sources and Wall Heat Transfer. J. Heat Transfer (Trans. A.S.M.E.), ser. C, vol. 81, no. 4, Nov. 1959, pp. 280-290.
19. Eckert, E. R. G.; and Drake, R. M., Jr.: Heat and Mass Transfer. Second ed., McGraw-Hill Book Co., Inc., 1959, p. 211.
20. Weiland, Walter F.; and Lowdermilk, Warren H.: Measurements of Heat-Transfer and Friction Coefficients for Air Flowing in a Tube of Length-Diameter Ratio of 15 at High Surface Temperatures. NACA RM E53E04, 1953.
21. Sparrow, E. M.; Hallman, T. M.; and Siegel, R.: Turbulent Heat Transfer in the Thermal Entrance Region of a Pipe with Uniform Heat Flux. Appl. Sci. Res., ser. A, vol. 7, no. 1, 1957, pp. 37-52.
22. Deissler, Robert G.: Analysis of Turbulent Heat Transfer, Mass Transfer and Friction in Smooth Tubes at High Prandtl and Schmidt Numbers. NACA Rept. 1210, 1955.
23. Siegel, R.; and Sparrow, E. M.: Comparison of Turbulent Heat-Transfer Results for Uniform Wall Heat Flux and Uniform Wall Temperature. J. Heat Transfer (Trans. A.S.M.E.), ser. C, vol. 82, no. 2, May 1960, pp. 152-153.
24. Simoneau, R. J.; and Hendricks, R. C.: A Simple Equation for Correlating Turbulent Heat Transfer to a Gas. Preprint No. 64-HT-36, ASME, 1964.
25. Petukhov, B. S.; and Popov, V. N.: Theoretical Calculation of Heat Exchange and Frictional Resistance in Turbulent Flow in Tubes of an Incompressible Fluid with Variable Physical Properties. High Temperature, vol. 1, no. 1, July-Aug. 1963, pp. 85-101.
26. Smith, J. M.: Introduction to Chemical Engineering Thermodynamics. McGraw-Hill Book Co., Inc., 1949.
27. Rossini, Frederick D.; Wagman, Donald D.; Evans, William H.; Levine, Samuel; and Jaffe, Irving: Selected Values of Chemical Thermodynamic Properties. Cir. No. 500, NBS, 1952, Table 18-2, Ser. 1.

28. Kelley, K. K.: Contributions to the Data on Theoretical Metallurgy. X. High-Temperature Heat-Content, Heat-Capacity, and Entropy Data for Inorganic Compounds. Bull. No. 476, Bur. Mines, 1949, pp. 3-6; 126.
29. Hougen, O. A.; and Watson, K. M.: Chemical Process Principles. Pt. 2 - Thermodynamics. John Wiley & Sons, Inc., 1947, ch. 16.
30. Brokaw, Richard S.: Alignment Charts for Transport Properties, Viscosity, Thermal Conductivity and Diffusion Coefficients for Nonpolar Gases and Gas Mixtures at Low Density. NASA TR R-81, 1960.
31. Hirschfelder, J. O.; Curtiss, C. F.; and Bird, R. B.: Molecular Theory of Gases and Liquids. John Wiley & Sons, Inc., 1954, ch. 8.
32. Beer, Hans: Wärmeübergang in Dissoziierenden Gasen. Institut für Thermodynamik der Flugtriebwerke Thesis, Technische Hochschule, Stuttgart (Germany), Mar. 1963.
33. Petker, Ira; and Mason, David M.: Viscosity of the  $N_2O_4$ - $NO_2$  Gas System. J. Chem. Eng. Data, vol. 9, no. 2, Apr. 1964, pp. 280-281.
34. Keyes, D. B.; and Deem, A. G.: Chemical Engineers Manual. John Wiley & Sons, Inc., 1942, p. 135.

TABLE I. - TEST CONDITIONS FROM VARIOUS DATA SOURCES

Source	Type	Boundary condition (a)	Tube length to diameter ratio, L/D	Heat flux $q$ , Btu/(hr)(sq ft)	Entrance Reynolds number, Re	Maximum local wall temperature, °K	Inlet pressure, atm
Reference 4	Experimental	UWT	81.2	4.1 to $6.5 \times 10^3$	12.0 to $20.0 \times 10^3$	375 to 387	1.0
Reference 8	Experimental	UHF	2	2.6 to 12.5	30.7 to 111	315 to 374	↓
Reference 9	Analytical	UHF	2	2.6 to 12.5	30.7 to 111	315 to 374	
Reference 5	Experimental	UWT	98.0	1.7 to 5.9	11.3 to 19.9	337 to 442	
Reference 6	Experimental	UWT	88.0	.3 to 8.4	6.7 to 22.0	311 to 477	↓
Reference 7	Experimental	UWT	16.0	.3 to 13.3	26.8 to 209	321 to 461	
Reference 10	Analytical	UHF	-----	-----	10.0 to 200	300 to 370	1.0
Reference 11	Experimental	UHF	184.0	.6 to 27.0	5.6 to 68.2	315 to 450	0.9 to 1.7
Present investigation	Experimental	UHF	39.6	6.2 to 44.2	18.9 to 135	359 to 572	1.6 to 2.1

<sup>a</sup>UWT = uniform wall temperature.  
UHF = uniform heat flux.

TABLE II. - EXPERIMENTAL CONDITIONS FOR N<sub>2</sub>O<sub>4</sub> SYSTEM

Run	Pressure, P, atm	Flow rate, W, lb/hr	Heat input, Q, Btu/hr	Bulk temperature rise, T <sub>b</sub> , °K	Maximum wall temperature, T <sub>w</sub> , °K	Heat balance error, percent
1	1.9	58.90	3995	344 to 365	562	11.1
2	1.9	53.20	4165	330 to 353	562	4.3
3	1.8	44.40	3960	314 to 343	562	2.6
4	1.8	34.00	3228	312 to 343	568	3.9
5	1.8	23.65	2422	312 to 345	572	5.2
6	1.7	14.80	1663	309 to 346	566	6.4
7	1.9	89.40	2808	318 to 329	359	14.9
8	1.7	64.10	2388	320 to 331	362	11.4
9	1.8	66.20	2148	320 to 330	359	8.8
10	1.8	67.40	2198	319 to 330	360	6.4
11	1.7	47.80	1846	316 to 329	360	4.5
12	1.6	31.30	1403	315 to 330	364	.2
13	1.6	17.93	874	313 to 329	361	3.0
14	2.0	115.8	6240	326 to 340	447	12.7
15	2.1	89.10	4750	325 to 342	440	1.5
16	2.1	75.50	4243	325 to 342	444	1.0
17	2.1	66.80	3836	325 to 343	445	2.8
18	2.1	46.20	2892	321 to 342	447	3.4

TABLE III. - SOME EXPERIMENTAL RESULTS FOR N<sub>2</sub>O<sub>4</sub> SYSTEM

Run	Mass average velocity, G, lb/(sq ft)(hr)	Uniform heat flux, q, Btu/(hr)(sq ft)	Fully developed enthalpy difference, $i_w - i_b$ , Btu/lb	Modified heat-transfer coefficient, $h'$ , lb/(sq ft)(hr)	Experimental modified Stanton number, $\frac{h'}{G}$	Inlet Reynolds number, Re
1	66 200	28 520	155.4	178	$2.69 \times 10^{-3}$	$61.3 \times 10^3$
2	59 760	29 530	195.7	151	2.53	60.4
3	49 900	28 080	229.0	123	2.46	55.3
4	38 200	22 880	232.4	98.3	2.58	42.9
5	26 580	17 170	229.3	74.6	2.81	29.9
6	16 630	11 790	227.3	51.9	3.12	18.9
7	100 400	19 910	104.0	192	1.91	108.7
8	72 000	16 940	98.96	171	2.38	77.1
9	74 400	15 230	93.91	162	2.18	79.8
10	75 750	15 690	95.59	163	2.15	81.6
11	53 720	13 080	100.9	130	2.42	58.6
12	35 180	9 945	107.3	93.4	2.65	38.6
13	20 140	6 196	102.3	60.6	3.01	22.4
14	130 100	44 250	175.1	253	1.94	135.1
15	100 100	33 680	174.9	192	1.92	104.6
16	84 800	30 100	176.3	171	2.02	88.8
17	75 050	27 200	175.8	155	2.07	78.6
18	51 920	20 520	182.1	113	2.18	55.4

TABLE IV. - EXPERIMENTAL WAVE  
 NUMBERS FOR THE NO<sub>2</sub> AND  
 N<sub>2</sub>O<sub>4</sub> MOLECULES

i	Wave number $\omega_i$ , cm <sup>-1</sup>	
	NO <sub>2</sub>	N <sub>2</sub> O <sub>4</sub>
1	648	283
2	1321	380
3	1621	380
4	-----	500
5	-----	500
6	-----	752
7	-----	0
8	-----	813
9	-----	1265
10	-----	1360
11	-----	1744
12	-----	1744

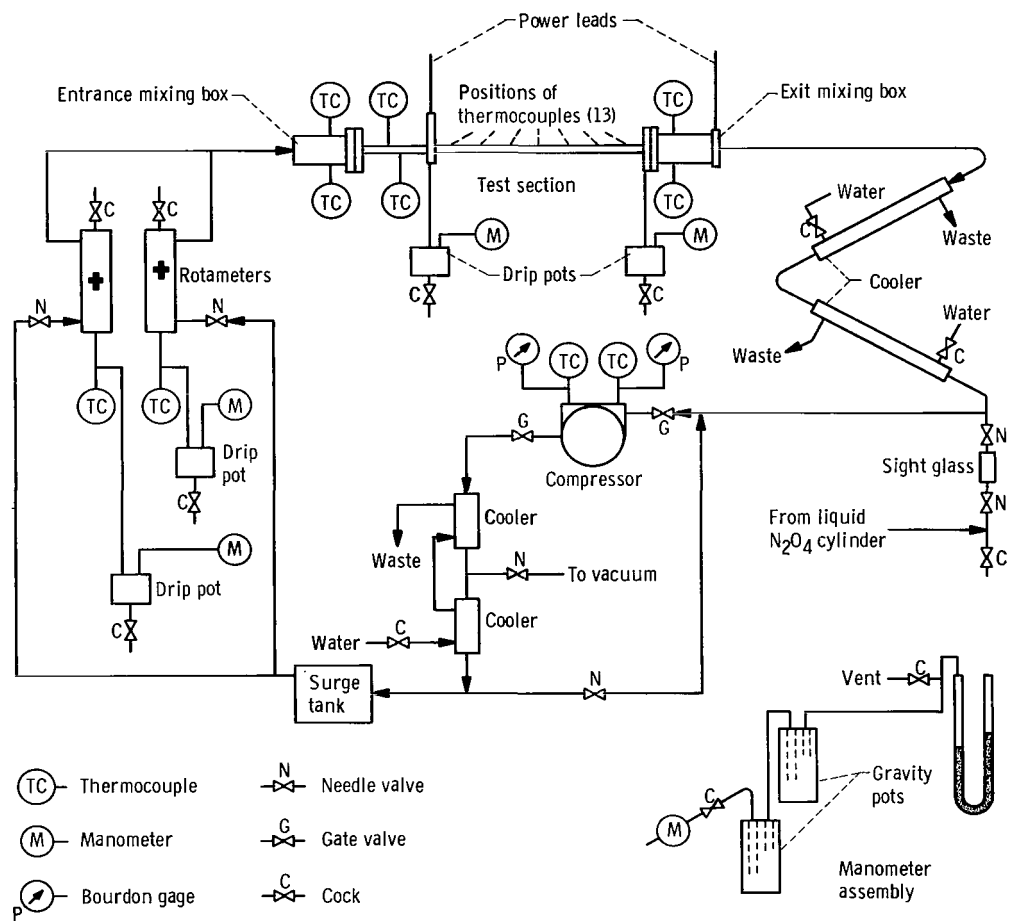
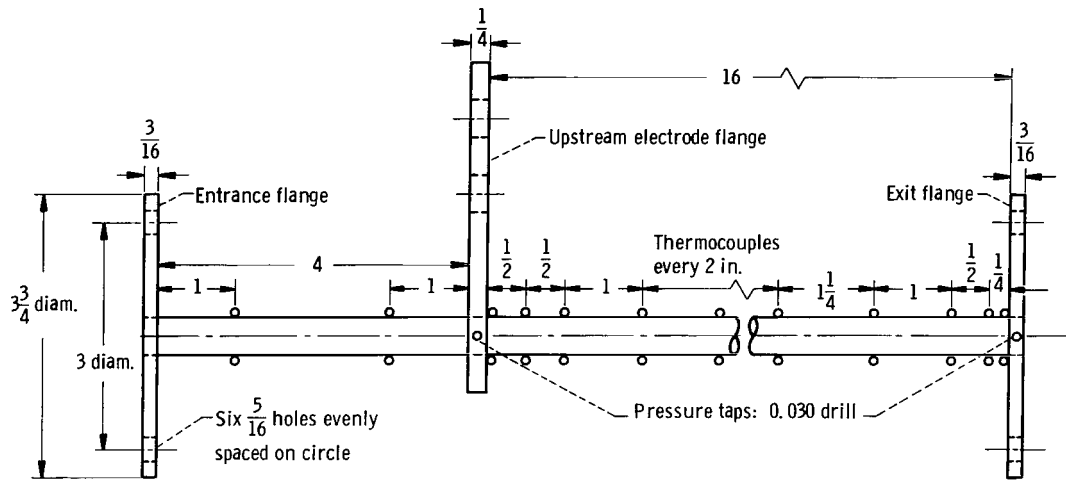
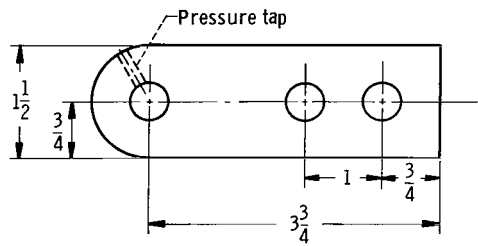


Figure 1. - Schematic of test loop.



(a) Test section.



(b) Upstream electrode flange.

Figure 2 - Test section detail and thermocouple location. (All units are inches.)

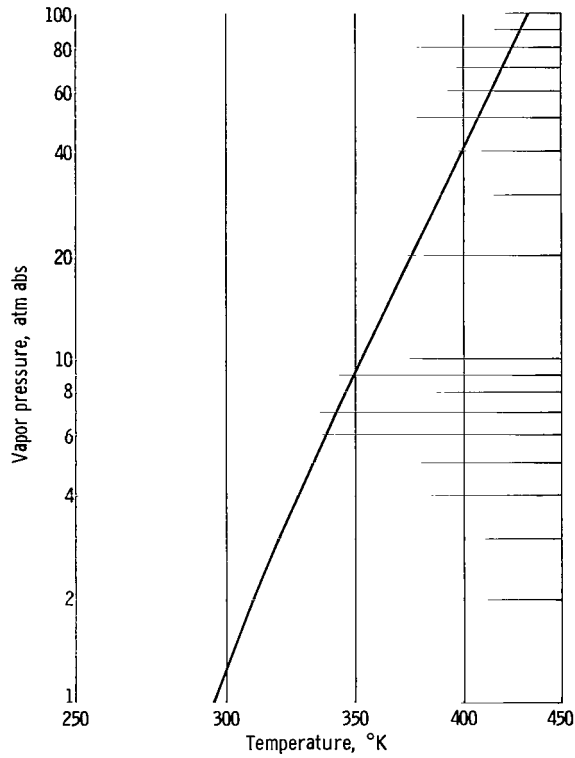


Figure 3. - Vapor pressure of liquid  $N_2O_4$ . Boiling point: 294.5° K, 1 atmosphere; critical point: 431.0° K, 99 atmospheres. (Data of ref. 34.)

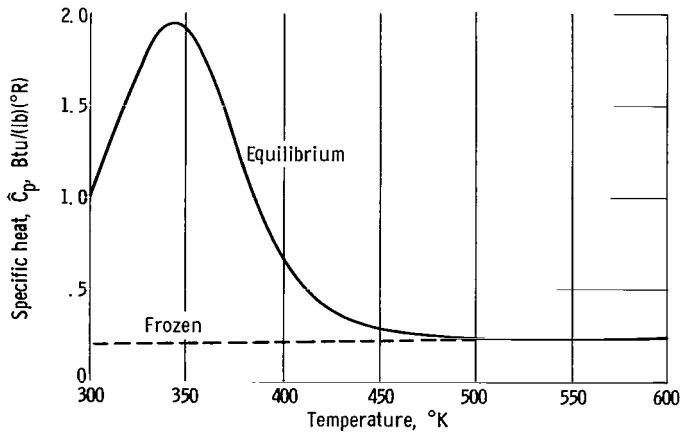


Figure 4. - Equilibrium and frozen specific heats as function of temperature for  $N_2O_4$  system. Absolute total pressure, 2 atmospheres.

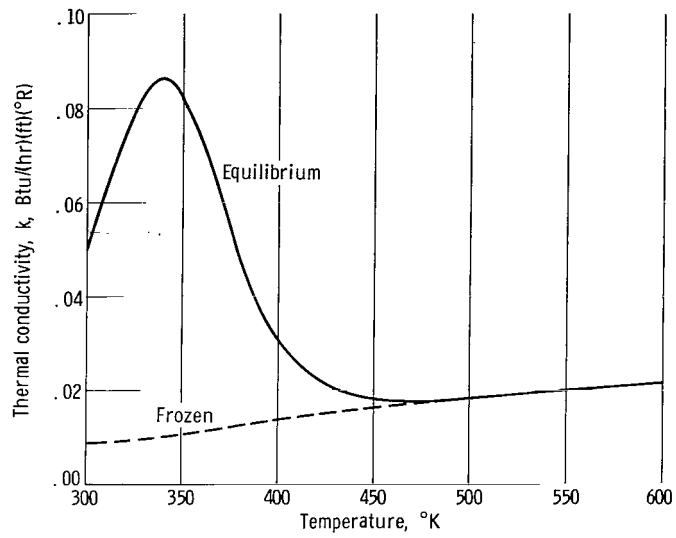


Figure 5. - Equilibrium and frozen thermal conductivities as function of temperature for  $N_2O_4$  system. Absolute total pressure, 2 atmospheres.

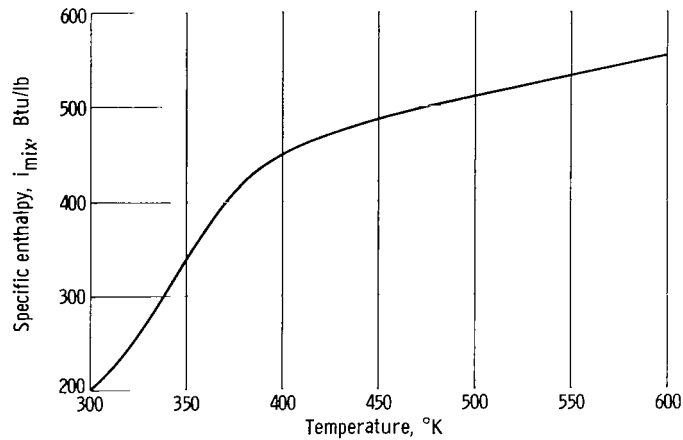


Figure 6. - Specific enthalpy as function of temperature for  $N_2O_4$  system. Absolute total pressure, 2 atmospheres.

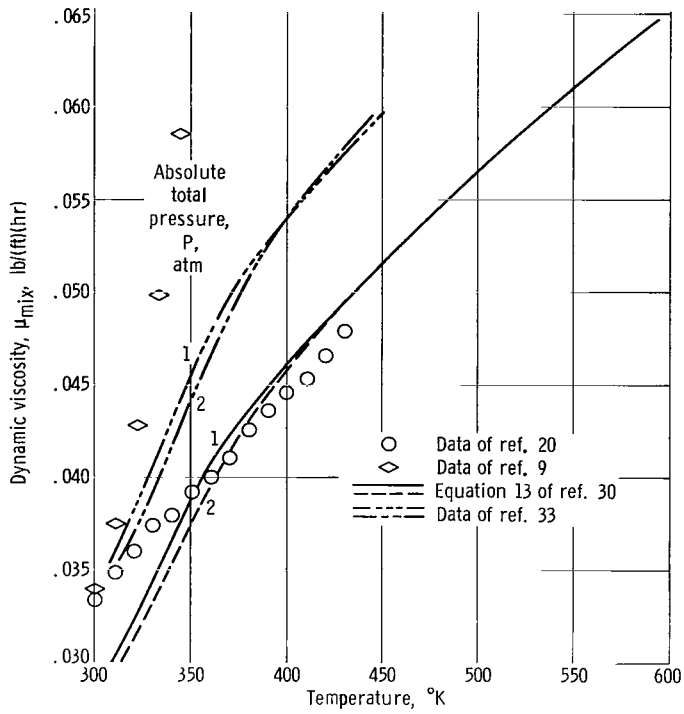


Figure 7. - Dynamic viscosity of  $N_2O_4 \rightleftharpoons 2NO_2$  system as function of temperature for absolute total pressures of 1 and 2 atmospheres.

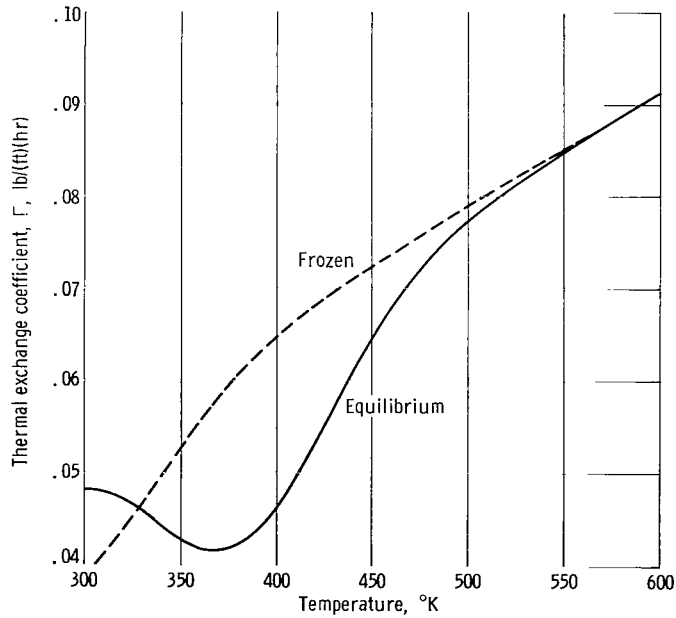


Figure 8. - Thermal exchange coefficient as function of temperature for  $N_2O_4$  system. Absolute total pressure, 2 atmospheres.

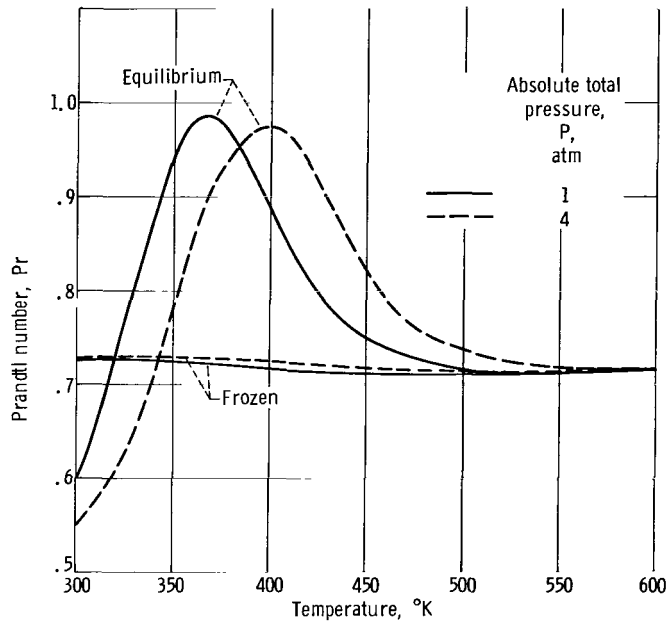


Figure 9. - Equilibrium and frozen property Prandtl numbers as function of temperature for  $N_2O_4$  system. Absolute total pressures, 1 and 4 atmospheres.

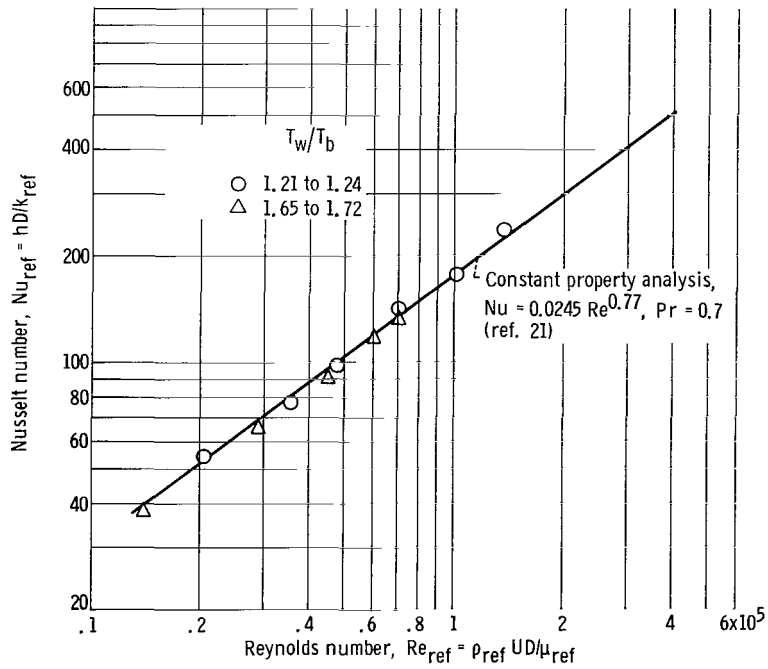


Figure 10. - Conventional heat-transfer correlation for air data. Properties evaluated at reference temperature  $T_{ref} = T_b + 0.5(T_w - T_b)$ .

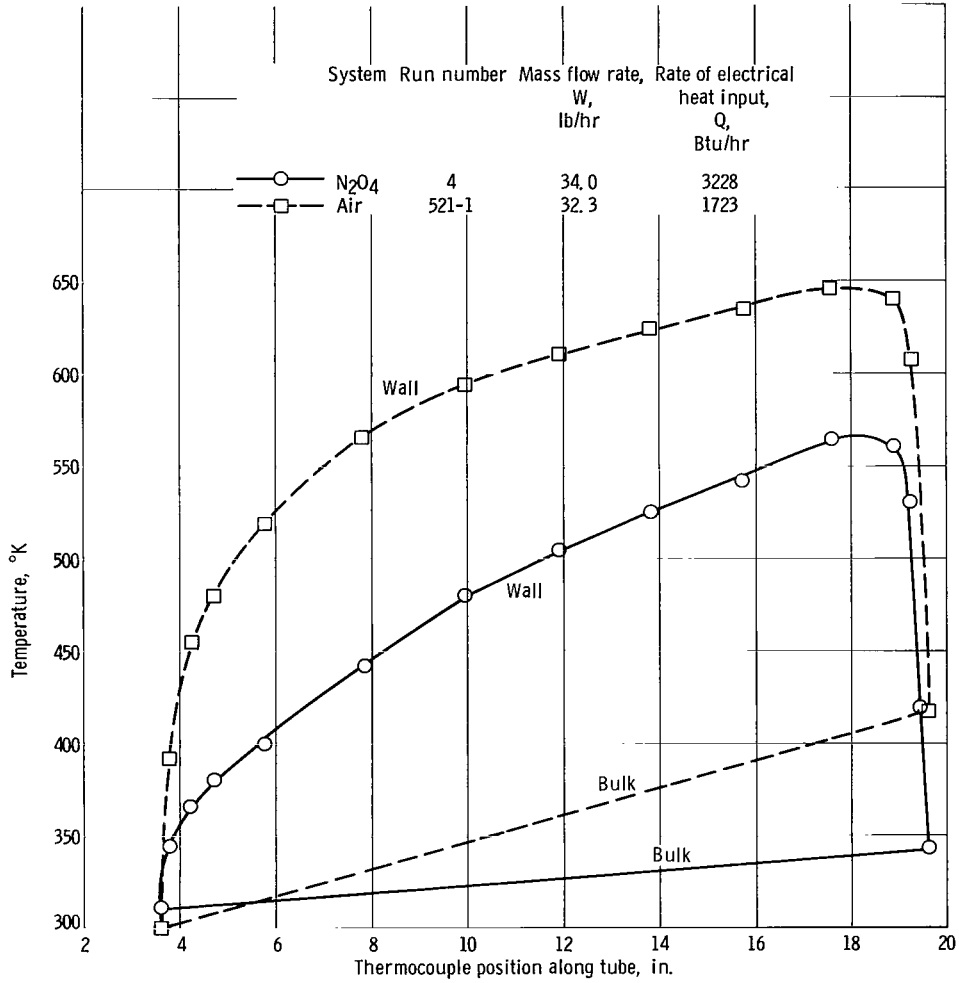


Figure 11. - Representative wall and bulk temperatures.

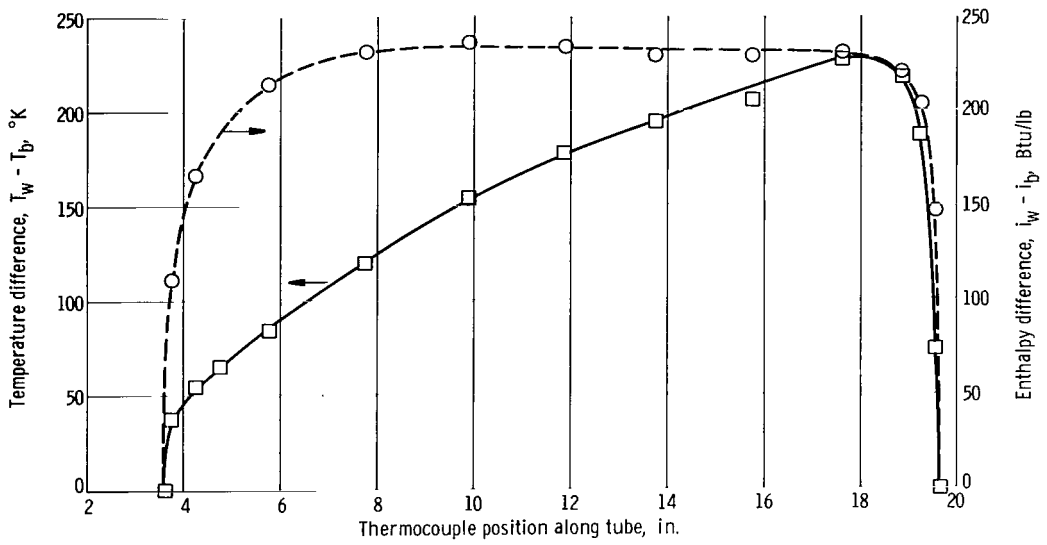


Figure 12. - Variation in wall- to bulk-enthalpy and temperature differences along tube for  $N_2O_4$  system. Run 4.

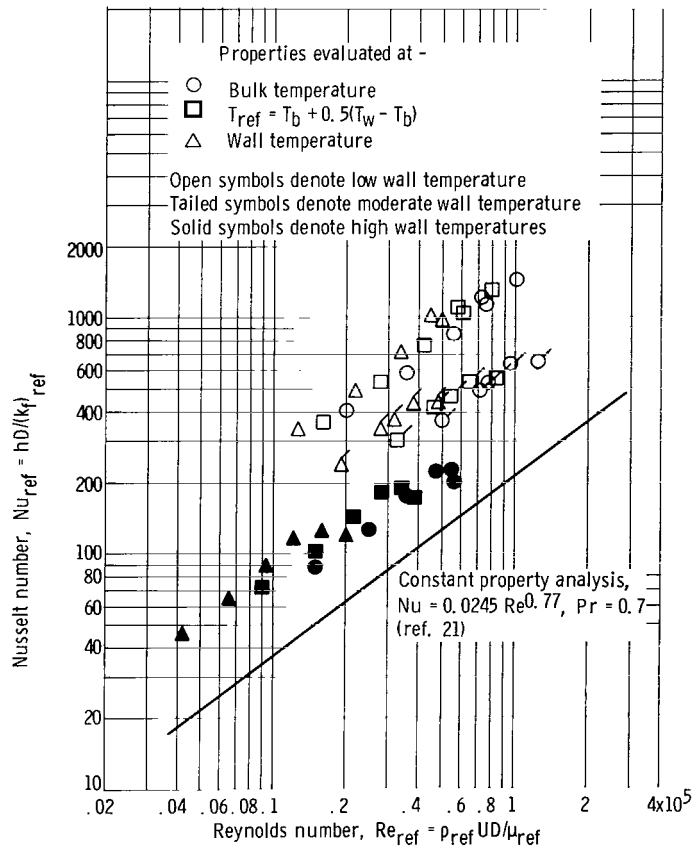


Figure 13. - Conventional heat-transfer correlation for  $N_2O_4$  system with frozen properties. Prandtl number  $Pr_f = 0.708$  to  $0.713$ .

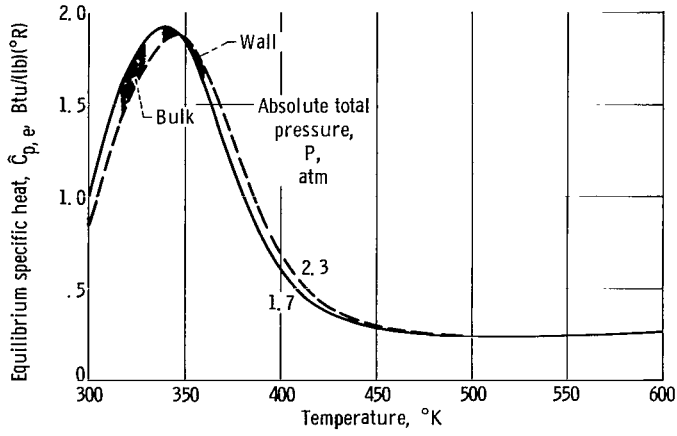


Figure 14. - Wall to bulk variation in equilibrium specific heat for low wall temperature runs in  $N_2O_4$  system. Runs 7 to 13.

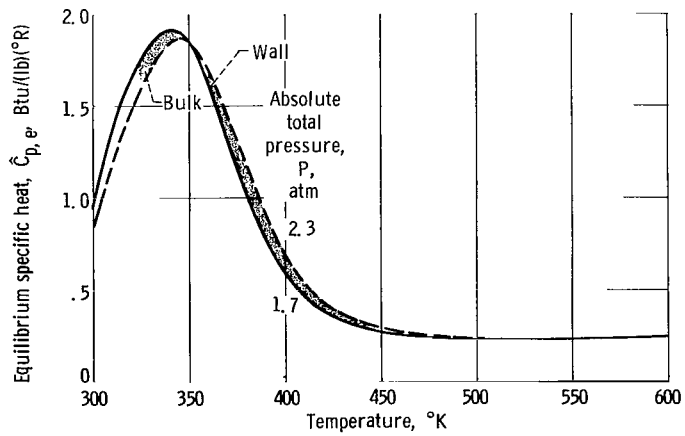


Figure 15. - Wall to bulk variation in equilibrium specific heat for intermediate wall temperature runs in  $N_2O_4$  system. Runs 14 to 18.

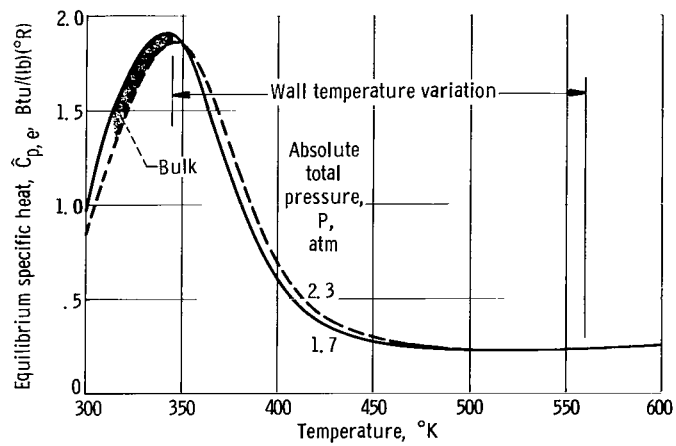


Figure 16. - Wall to bulk variation in equilibrium specific heat for high wall temperature runs in  $N_2O_4$  system. Runs 1 to 6.

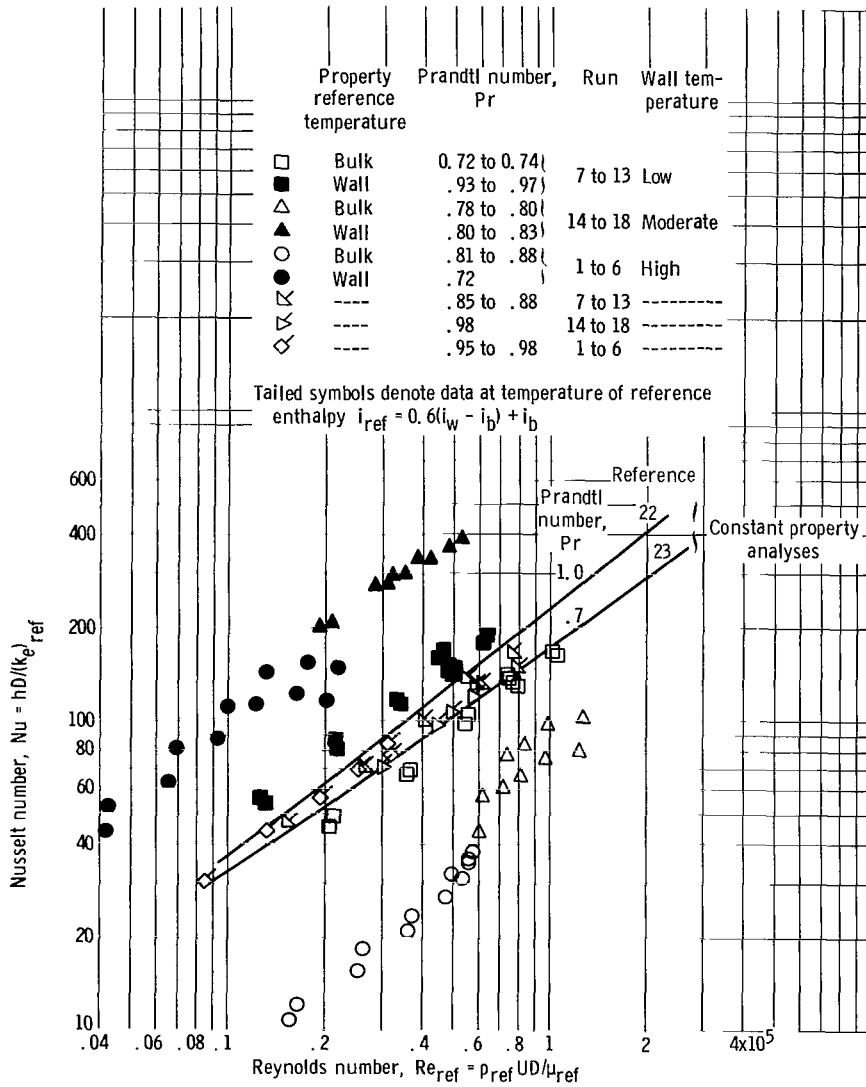


Figure 17. - Conventional heat-transfer correlation of  $N_2O_4$  data with equilibrium properties.

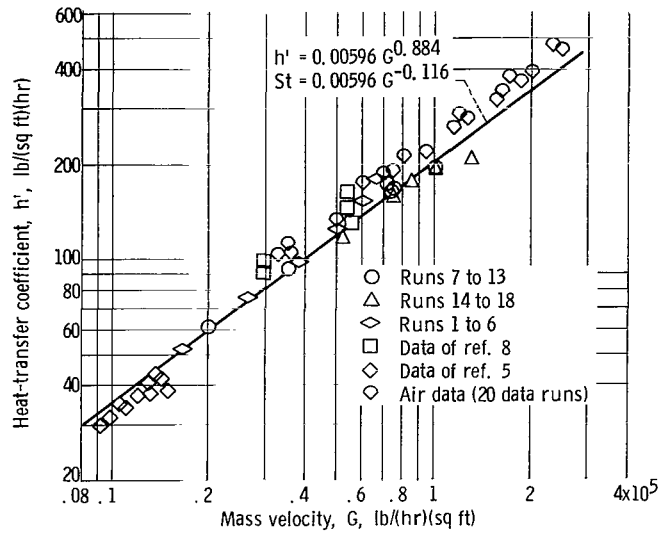


Figure 18. - Basic correlation of several  $N_2O_4$  heat-transfer experiments.

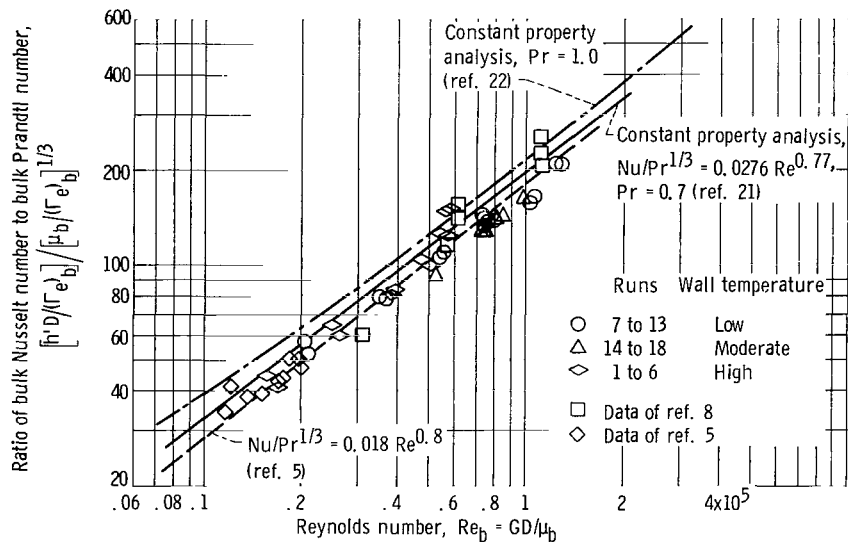


Figure 19. - Data correlation for  $N_2O_4$  system with bulk properties.

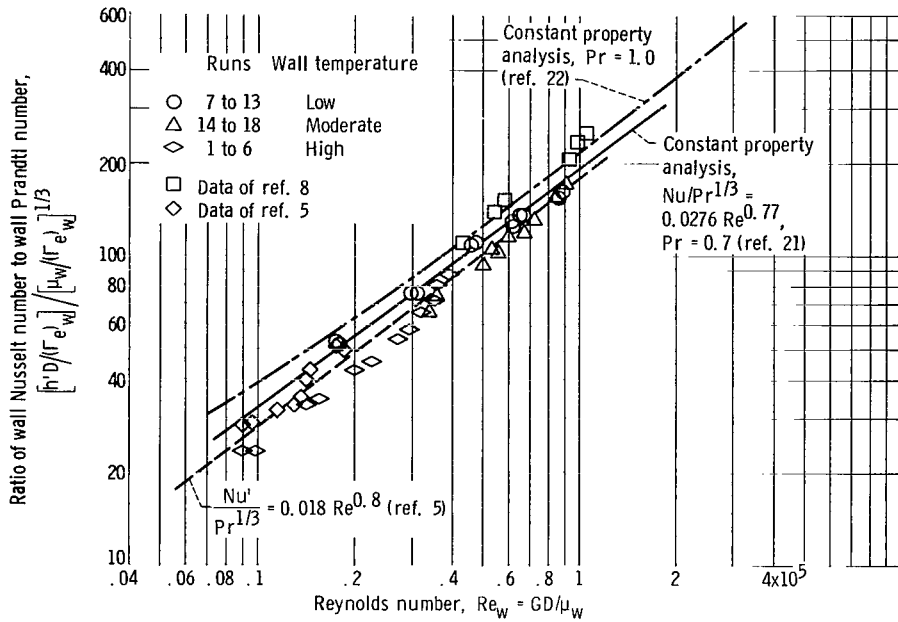


Figure 20. - Data correlation for  $N_2O_4$  system with wall properties.

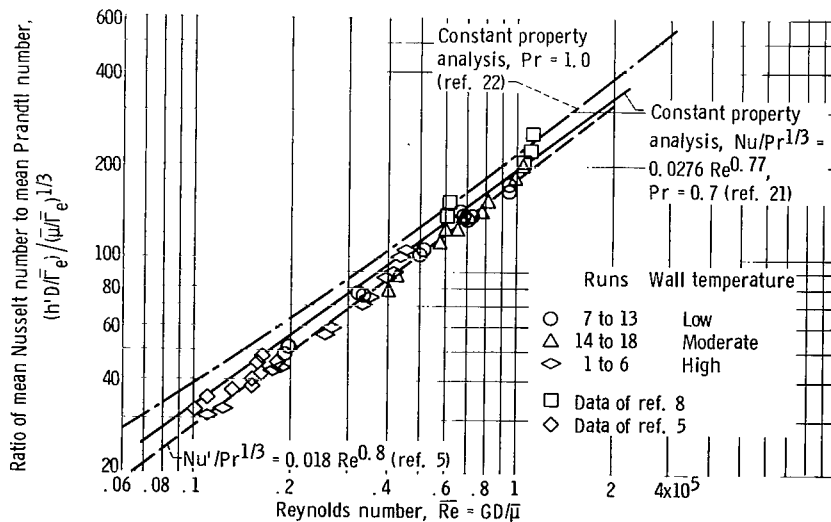


Figure 21. - Data correlation for  $N_2O_4$  system with integral mean properties.

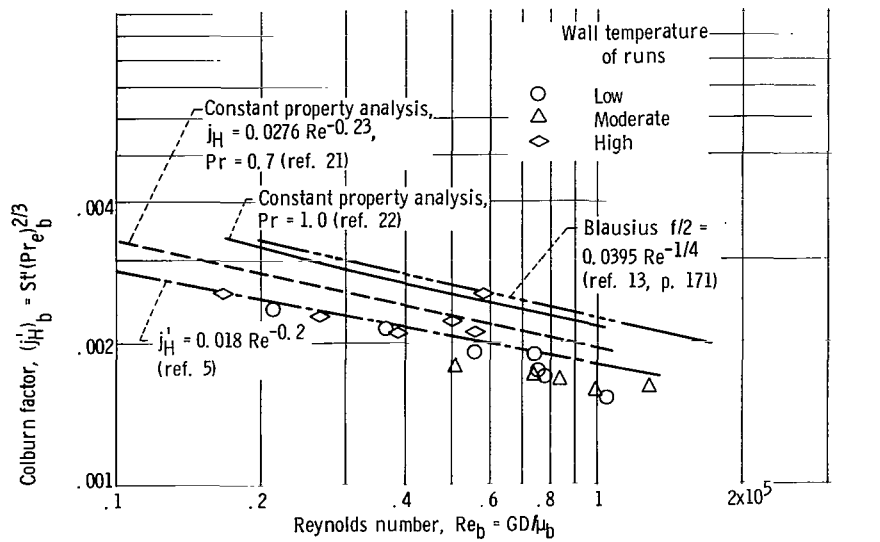


Figure 22. - Correlation of  $N_2O_4$  data by Colburn analogy. Properties evaluated at bulk temperatures.

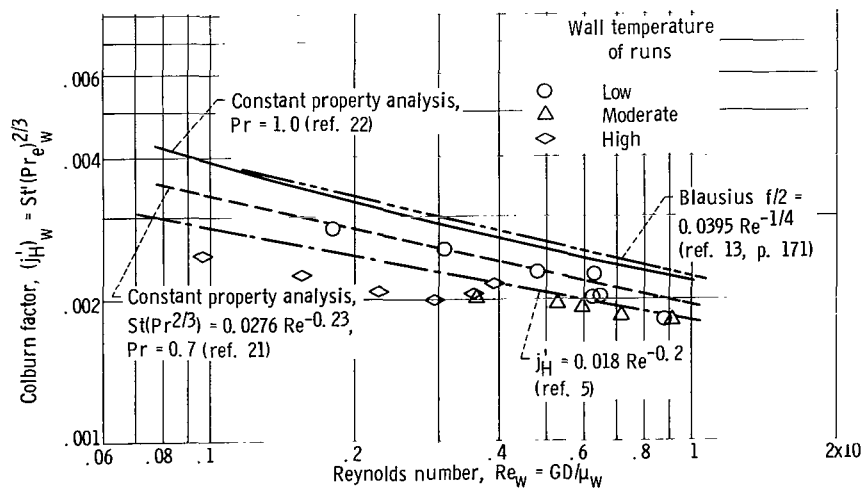


Figure 23. - Correlation of  $N_2O_4$  data by Colburn analogy. Properties evaluated at wall temperatures.

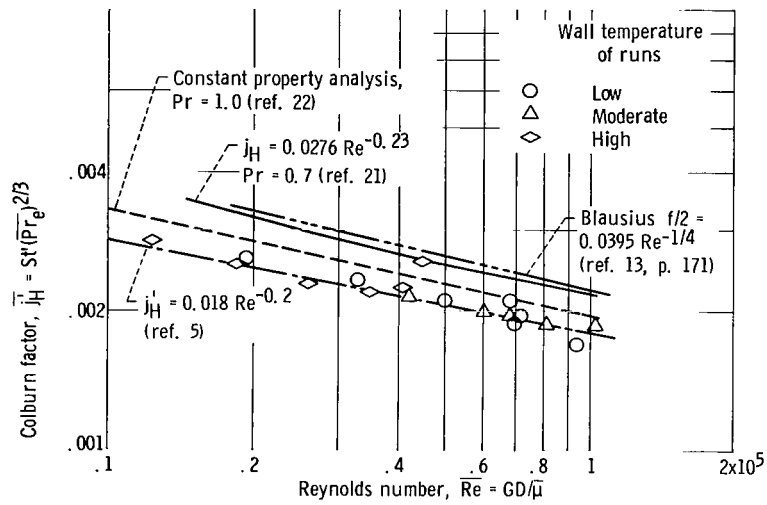


Figure 24. - Correlation of  $N_2O_4$  data by Colburn analogy. Properties evaluated at integral mean.

*"The aeronautical and space activities of the United States shall be conducted so as to contribute . . . to the expansion of human knowledge of phenomena in the atmosphere and space. The Administration shall provide for the widest practicable and appropriate dissemination of information concerning its activities and the results thereof."*

—NATIONAL AERONAUTICS AND SPACE ACT OF 1958

## NASA SCIENTIFIC AND TECHNICAL PUBLICATIONS

**TECHNICAL REPORTS:** Scientific and technical information considered important, complete, and a lasting contribution to existing knowledge.

**TECHNICAL NOTES:** Information less broad in scope but nevertheless of importance as a contribution to existing knowledge.

**TECHNICAL MEMORANDUMS:** Information receiving limited distribution because of preliminary data, security classification, or other reasons.

**CONTRACTOR REPORTS:** Technical information generated in connection with a NASA contract or grant and released under NASA auspices.

**TECHNICAL TRANSLATIONS:** Information published in a foreign language considered to merit NASA distribution in English.

**TECHNICAL REPRINTS:** Information derived from NASA activities and initially published in the form of journal articles.

**SPECIAL PUBLICATIONS:** Information derived from or of value to NASA activities but not necessarily reporting the results of individual NASA-programmed scientific efforts. Publications include conference proceedings, monographs, data compilations, handbooks, sourcebooks, and special bibliographies.

*Details on the availability of these publications may be obtained from:*

SCIENTIFIC AND TECHNICAL INFORMATION DIVISION  
NATIONAL AERONAUTICS AND SPACE ADMINISTRATION  
Washington, D.C. 20546